Studies on the Role of Oxidative Stress in Mutagenesis by Using *Nrf2*-deficient Mice

（*Nrf2* 欠損マウスを用いた変異原性における酸化ストレスの役割に関する研究）

2018

The United Graduate School of Veterinary Sciences, Gifu University

(Gifu University)

TSUCHIYA, Takuma

Studies on the Role of Oxidative Stress in Mutagenesis by Using *Nrf2*-deficient Mice

（*Nrf2* 欠損マウスを用いた変異原性における酸化ストレスの役割に関する研究）

TSUCHIYA, Takuma

Contents

Abbreviations

6-TG:	6-thioguanine
6-TG^{R}:	6-thioguanine resistant
8-OHdG:	8-hydroxydeoxyguanosine
ARE:	antioxidant response element
BER:	base excision repair
BW:	body weight
bp:	base pair
Cm^{R}:	chloramphenicol resistant
DSBs:	double-strand breaks
E. coli:	*Escherichia coli*
GST:	glutathione *S*-transferase
HO1:	heme oxygenase 1
$KBrO_3$:	potassium bromate
KEAP1:	Kelch-like ECH-associated protein 1
MFs:	mutant frequencies
MW:	molecular weight
NFA:	5-nitro-2-furaldehyde
NFT:	nitrofurantoin
NRF2:	nuclear factor erythroid 2-related factor 2
Nrf2$^{+/+}$:	*Nrf2*-proficient
Nrf2$^{-/-}$:	*Nrf2*-deficient

NQO1:	NAD(P)H:quinone oxidoreductase 1
PCR:	polymerase chain reaction
ppm:	parts per million
ROS:	reactive oxygen species
SD:	standard deviation
SDS-PAGE:	SDS-polyacrylamide gel electrophoresi
TBARS:	thiobarbituric acid-reactive substances

General Introduction

Since there are many carcinogenic substances in the environment: medicines, industrial products, mold poisons, air pollutants, and food additives, we are always in danger of them. The assessment of carcinogenesis risk in chemical substances such as food additives and residual pesticides which are ingested by humans through the diet is one of the most important issues for the public health. Carcinogenic substances are classified by their mechanisms into two types: one is genotoxic carcinogens and another is non-genotoxic carcinogens. Genotoxic carcinogens have no threshold because of the direct action to DNA. The risk of these carcinogens is thought to be very severe (10, 41). On the other hand, non-genotoxic carcinogens exert their carcinogenic potential through the effects to the proliferation, enzymes, oxidative stress, and so on, and they are thought to have each threshold (11). For these reasons, clarifying the mechanisms of non-genotoxic carcinogens is necessary for their risk assessment.

Recently, oxidative stress is well known as a key factor of chemical carcinogenesis. A lot of types of the role of oxidative stress in chemical carcinogenesis have been demonstrated in many studies. Oxidative stress involves in chemical carcinogenesis as a promoter in so-called two-step carcinogenesis model by stimulating the proliferation of initiated cells (29, 37, 44). On the other hand, oxidative stress might act as an initiator (37, 42, 45, 57). While repairing the oxidative DNA damages which is formed by the chemical-induced reactive oxygen species (ROS), the error of repair of these lesions can lead to gene mutations (38, 39). The renal tubule in the kidney is a main target of oxidative stress. The kidney is exposed to many chemical substances

during excretion and reabsorption, and redox cycles act vigorously accompanied with the production of ROS in the process (47, 60). Therefore, oxidative stress is considered to take a crucial role in renal carcinogenesis.

Gpt delta rats and mice are the transgenic animal models which can detect *in vivo* mutagenicity in the target organs. In the animals, lambda EG10 DNA derived from *Escherichia. coli* is transfected, and the chemical-induced mutations in the DNA in each target organ are evaluated. *In vivo* mutation assay is consists of 6-thioguanine (6-TG) and Spi$^-$ selection, which can detect point mutation and deletion mutation, respectively (34, 40). This animal model can play an important role in the investigation about the mechanism and risk of chemical-induced carcinogenesis in rodents. Actually, our previous studies have clarified *in vivo* mutagenicity in environmental carcinogenic substances (27, 34, 55).

The redox-sensitive transcription factor nuclear factor erythroid 2-related factor 2 (NRF2) regulates cellular responses to oxidative stress in cooperation with Kelch-like ECH-associated protein 1 (KEAP1). Oxidative stress causes translocation of NRF2 from cytoplasm into the nucleus, where it can bind to the antioxidant response element (ARE) and consequently transactivate ARE-bearing genes encoding anti-oxidant-related enzymes (23, 32). In this way, NRF2-ARE pathway protects cells from oxidative stress. Thus, *Nrf2*-deficient (*Nrf2*$^{-/-}$) mice show high-sensitivity to oxidative stress, and they play a role in the investigation of involvement of oxidative stress in chemical-induced toxicity. In addition, *Nrf2*$^{-/-}$ *gpt* delta mice created from *Nrf2*$^{-/-}$ mice and *gpt* delta mice which can detect *in vivo* mutagenicity through 6-thioguanine (6-TG) and Spi$^-$ selection

are new useful tools in the research for the role of oxidative stress in chemical-induced mutagenesis.

Nitrofurantoin (NFT), an antimicrobial compound, and potassium bromate ($KBrO_3$), a food additive developed as a flour treatment agent, are chemical substances potentially ingested by humans through food. However, they both induce renal tumor in rats, and are prohibited or restricted in use currently for the concern about carcinogenesis risk in humans (9, 13, 18, 20, 21). At the same time, the oxidative stress-inducing potential is suspected from their chemical structure. NFT and $KBrO_3$ have a nitro group and bromate ion, respectively. Reduction of nitro group might induce oxidative stress, and bromate ion has a potential as an oxidant agent. For these reasons, the involvement of oxidative stress is suspected in their renal carcinogenesis (1, 2, 3, 4, 26, 56, 59).

8-hydroxydeoxyguanosine (8-OHdG) is the fairly stable and the most abundant oxidized DNA lesion induced by ROS (25), and is frequently used as a biomarker of oxidative stress in humans and experimental animals (5, 19, 27, 50, 58, 62). In humans and animals, repair of 8-OHdG is performed by the base excision repair (BER) enzymes such as OGG1, MUTYH and MTH1 (35). Mispairing of the remained 8-OHdG through BER process with adenine base results in G:C–T:A transversion mutations (38, 39). The error during the repair of 8-OHdG also causes deletion mutations (55). These actions concerning 8-OHdG suggest the important role of 8-OHdG in the chemical-induced mutagenicity. In fact, our previous studies showed the elevation of mutation frequency

accompanied with the increase of 8-OHdG level in the kidney of NFT or $KBrO_3$-treated *gpt* delta rats (27, 55).

The aim of the present study is the investigation about the involvement of oxidative stress in NFT or $KBrO_3$-induced *in vivo* mutagenicity. To attain the objective, I used *Nrf2*$^{-/-}$ *gpt* delta mice which lack the defense mechanisms against oxidative stress and can detect *in vivo* mutagenicity, and performed the reporter gene mutation assays and measurements of 8-OHdG levels in their kidney. In chapter 1, I elucidated the relationship between oxidative stress-related mutagenicity induced by NFT and the chemical structure. NFT is synthesized by the condensation of 5-nitro-2-furaldehyde (NFA), a basic skeleton containing a nitro group, and 1-aminohydantoin, a side chain. Because the relationship between NFT-induced oxidative stress and its chemical structure remains unclear in our previous study about NFT and its moieties using *gpt* delta rats (27), I performed the additional consideration using *Nrf2*$^{-/-}$ *gpt* delta mice. In chapter 2, I investigated the relationship between the formation of 8-OHdG and subsequent several types of gene mutations. Even though NFT and $KBrO_3$ induce the elevation of mutation frequency accompanied with the increase of 8-OHdG level in the kidney as previously mentioned (27, 55), the characteristic mutation pattern is different for each. NFT induces guanine base transversion mutations (27), and $KBrO_3$ induces deletion mutations (55). Thus, I used *Nrf2*$^{-/-}$ *gpt* delta mice for the investigation about the relationship between 8-OHdG and subsequent gene mutations.

Chapter 1

Role of oxidative stress in the chemical structure-related genotoxicity of nitrofurantoin in *Nrf2*-deficient *gpt* delta mice

Introduction

Nitrofurans are antimicrobial compounds that contain a nitro group at the 5-position of the furan ring and an amine or hydrazide side chain derivative (Fig. 1). Some nitrofurans are prohibited from use in veterinary medicine in Japan owing to their genotoxic and carcinogenic potential (15, 16, 17, 18). However, new nitrofurans with various hydrazide derivatives on the side chain are being developed, given their easy synthesis and high antimicrobial activity (8, 63). Therefore, it is necessary to clarify the chemical structure-related genotoxicity of nitrofurans to facilitate risk assessments for human applications.

One nitrofuran group, nitrofurantoin (NFT), is synthesized by the condensation of 5-nitro-2-furaldehyde (NFA) (Fig. 1) and 1-aminohydantoin and is a renal carcinogen in rats (9). The formation of reactive oxygen species (ROS) or intermediates resulting from the reduction of the nitro group of NFT is thought to exert antibacterial activity (2, 3, 4). Accordingly, we hypothesized that oxidative stress is involved in NFT-induced renal carcinogenesis. We recently demonstrated significant increases in the levels of 8-hydroxydeoxyguanosine (8-OHdG), an oxidized DNA lesion, and *gpt* mutant frequencies (MFs) with substitutions at guanine bases in the kidneys of *gpt* delta rats treated with NFT (27). However, the 1-aminohydantoin side-chain did not increase 8-OHdG levels or *gpt* MFs (27). NFA containing a nitro group, similar to NFT, did not increase 8-OHdG levels, but increased *gpt* MFs in the kidneys of *gpt* delta rats with different mutation spectra from those for NFT (27). Accordingly, the relationship between NFT-induced oxidative stress and its chemical structure remains unclear (27).

The redox-sensitive transcription factor nuclear factor erythroid 2-related factor 2 (NRF2) regulates cellular responses to oxidative stress. NRF2 is anchored in the cytoplasm by Kelch-like ECH-associated protein 1 (KEAP1), which also mediates the proteasomal degradation of NRF2. Oxidative stress causes the dissociation of NRF2 from KEAP1 and leads to NRF2 translocation into the nucleus, where it can bind to the antioxidant response element (ARE) and consequently transactivate ARE-bearing genes encoding anti-oxidant-related enzymes, such as NAD(P)H:quinone oxidoreductase 1 (NQO1), heme oxygenase 1 (HO1), and glutathione *S*-transferase (GST) (23, 32). Thus, the NRF2-ARE pathway has broad protective effects against oxidative stress. *Nrf2*-deficient mice clearly show greater sensitivity to various toxicants, as evidenced by the induction of the oxidative stress response following exposure to acetaminophen, 4-vinylcyclohexene diepoxide, pentachlorophenol, 2-amino-3-methylimidazo[4,5-f]quinoline, ferric nitrilotriacetate, and piperonylbutoxide (7, 14, 24, 28, 50, 58, 62).

In the present study, the role of oxidative stress in the chemical structure-related genotoxicity of NFT was determined using *Nrf2*-proficient and -deficient mice exposed to NFT or NFA for 13 weeks, followed by reporter gene mutation assays (34, 40) and measurements of 8-OHdG levels in the kidney.

Materials and Methods

Chemicals

NFT ($C_8H_6N_4O_5$, MW 238.2, CAS No. 67-20-9) and NFA ($C_5H_3NO_4$, MW 141.08, CAS No. 698-63-5) were purchased from Sigma-Aldrich Co. (St. Louis, MO, USA) and were suspended in 0.5 w/v% methyl cellulose 400 cP solution (Wako Pure Chemical Industries, Ltd., Osaka, Japan). Suspensions of the test chemicals were used at a volume of 10 mL/kg body weight (BW), based on BW on the day of chemical administration to *Nrf2*$^{+/+}$ or *Nrf2*$^{-/-}$ *gpt* delta mice.

Animals, diet, and housing conditions

The study protocol was approved by the Animal Care and Utilization Committee of the National Institute of Health Sciences. *Nrf2*-deficient mice with the C57BL/6J background established by Itoh *et al.* (22), were crossed with *gpt* delta mice with the C57BL/6J background (Japan SLC, Shizuoka, Japan). *Nrf2*$^{-/-}$ *gpt* delta mice and *Nrf2*$^{+/+}$ *gpt* delta mice were then obtained from the F1 generation and genotyped by polymerase chain reaction (PCR) with DNA collected from the tail of each mouse. All mice were housed in polycarbonate cages (5 mice per cage) with hard wood chips for bedding in a conventional animal facility maintained at a controlled temperature (23 ± 2°C) and humidity (55 ± 5%), with 12 air changes per hour, and a 12-h light/dark cycle. Mice were given free access to the CRF-1 basal diet (Charles River Japan, Kanagawa, Japan) and tap water.

Experimental design

Experimental design is described in Fig. 2. Eight-week-old male mice of each genotype were divided into five groups (four or five mice per group), i.e., two groups each administered NFT and NFA by gavage for five consecutive days and a control group administered vehicle alone. For daily doses, 70 and 35 mg/kg NFT were used. NFT at 70 mg/kg was the maximum tolerated dose in a preliminary dose selection study. NFA was set to 41 and 21 mg/kg, the same molar doses used for NFT. BW was measured every week. At necropsy, animals were killed by exsanguination under isoflurane (Mylan Inc., Tokyo, Japan) anesthesia, and the bilateral kidneys were collected and weighed. A portion of the kidney tissues was frozen with liquid nitrogen and stored at -80°C for the *in vivo* mutation assay, 8-OHdG measurements, and western blotting. A part of collected kidney was homogenized in ISOGEN (Nippon Gene, Tokyo, Japan) and stored at -80°C until use for the isolation of total RNA.

RNA isolation and quantitative real-time PCR for mRNA expression

Total RNA was extracted using ISOGEN according to the manufacturer's instruction. cDNA copies of total RNA were obtained using a High Capacity cDNA Reverse Transcription Kit (Life Technologies).

All PCRs were performed using the Applied Biosystems 7900HT FAST Real-Time PCR System with primers for mouse *Nqo1* obtained from TaqMan® Gene Expression Assays and TaqMan® Rodent GAPDH Control Reagents. Expression levels were calculated by the relative standard curve method and were determined relative to

Gapdh levels. Data are presented as fold-change values of treated samples relative to controls.

Protein extraction, SDS-PAGE, and western blotting

The kidneys from all animals were homogenized using a Teflon homogenizer with ice-cold RIPA lysis buffer (Wako Pure Chemical Co.) containing mammalian protease inhibitor cocktail. Samples were homogenized and centrifuged at 15,000 × *g* for 30 min, and the resulting supernatants were used. Protein concentrations were determined using the Advanced Protein Assay (Cytoskeleton, Denver, CO, USA) with bovine serum albumin as a standard. Samples were separated by SDS-polyacrylamide gel electrophoresis (SDS-PAGE) and transferred to 0.45-μm PVDF membranes (Millipore, Billerica, MA, USA). For the detection of target proteins, membranes were incubated with an anti-NQO1 polyclonal antibody (1:1000; Abcam, Cambridge, UK) and anti-β-actin monoclonal antibody (1:3000; Abcam) at 4°C overnight. Secondary antibody incubation was performed using horseradish peroxidase-conjugated secondary anti-rabbit or anti-mouse antibody at room temperature. Protein detection was facilitated by chemiluminescence using ECL Plus (GE Healthcare Japan Ltd., Tokyo, Japan).

Measurement of 8-OHdG

Renal DNA of *Nrf2*$^{-/-}$ *gpt* delta mice and *Nrf2*$^{+/+}$ *gpt* delta mice was extracted and digested as described previously (54). Briefly, nuclear DNA was extracted using a DNA Extractor WB Kit (Wako Pure Chemical Co.). To prevent artefactual oxidation in

the cell lysis step, deferoxamine mesylate (Sigma Chemical) was added to the lysis buffer. DNA was digested to deoxynucleotides by treatment with nuclease P1 and alkaline phosphatase using the 8-OHdG Assay Preparation Reagent Kit (Wako Pure Chemical Co.). The levels of 8-OHdG (8-OHdG/10^5 dG) were measured by high-performance liquid chromatography using an electrochemical detection system (Coulochem II; ESA, Bedford, MA, USA) as previously reported (55).

In vivo mutation assays

6-Thioguanine (6-TG) and Spi^- selection were performed using the methods described by Nohmi *et al.* (40). Briefly, genomic DNA was extracted from the kidneys of animals in each group using the RecoverEase DNA Isolation Kit (Agilent Technologies, Santa Clara, CA, USA), and lambda EG10 DNA (48 kb) was rescued as phages by *in vitro* packaging using Transpack Packaging Extract (Agilent Technologies). For 6-TG selection, packaged phages were incubated with *Escherichia coli* YG6020, which expresses Cre recombinase, and converted to plasmids carrying *gpt* and chloramphenicol acetyltransferase genes. Infected cells were mixed with molten soft agar and poured onto agar plates containing chloramphenicol and 6-TG. To determine the total number of rescued plasmids, infected cells were also poured on plates containing chloramphenicol without 6-TG. The plates were then incubated at 37°C for selection of 6-TG-resistant colonies, and the *gpt* MF was calculated by dividing the number of *gpt* mutants after clonal correction by the number of rescued phages. The *gpt* mutations were characterized by the amplification of a 739-bp DNA fragment

containing the 456-bp coding region of the *gpt* gene (40) and sequencing the PCR products using an Applied Biosystems 3730*xl* DNA Analyzer (Life Technologies Corporation, Carlsbad, CA, USA). For Spi$^-$ selection, packaged phages were incubated with *E. coli* XL-1 Blue MRA for survival titration and *E. coli* XL-1 Blue MRA P2 for mutant selection. Infected cells were mixed with molten lambda-trypticase agar plates. The next day, plaques (Spi$^-$ candidates) were punched out with sterilized glass pipettes and the agar plugs were suspended in SM buffer. The Spi$^-$ phenotype was confirmed by spotting the suspensions on three types of plates where the XL-1 Blue MRA, XL-1 Blue MRA P2, or WL95 P2 strain was spread on soft agar. Spi$^-$ mutants forming clear plaques on every plate were counted.

Statistical analysis

Data are presented as mean ± standard deviation (SD). Statistical analyses of differences in BW, kidney weights, 8-OHdG levels, mRNA expression levels, *gpt* and Spi$^-$ MFs, and *gpt*-mutation spectra between values of the control group from mice of the same genotype were analyzed by Dunnett's multiple comparison test. Comparison between mRNA expression levels of each control group of *Nrf2*-proficient and -deficient mice were made using the Student's *t*-test. $P < 0.05$ was considered significant.

Results

Body and kidney weights

Body and kidney weights of *Nrf2*-proficient and -deficient mice treated with NFT or NFA for 13 weeks are summarized in Fig. 3 and Table 1. For both genotypes, there were no significant differences in body and kidney weights between treated and untreated mice.

Quantitative real-Time PCR and western blotting analyses of Nqo1

For both genotypes, the mRNA expression level of *Nqo1* was not significantly influenced by NFT or NFA treatment. In *Nrf2*-deficient mice, however, the *Nqo1* mRNA expression level was significantly lower than that in *Nrf2*-proficient mice (Fig. 4A).

Furthermore, at the protein expression level, NQO1 was not affected by NFT or NFA treatment. In *Nrf2*-deficient mice, however, the NQO1 protein expression level was lower than that in *Nrf2*-proficient mice (Fig. 4B).

8-OHdG levels in kidney DNA

8-OHdG levels in *Nrf2*-deficient mice treated with 70 mg/kg NFT were significantly higher than those in control mice. 8-OHdG levels in *Nrf2*-deficient mice treated with NFA showed the tendencies of increase in a dose-dependent manner although they were not statistically significant because of insufficiency of samples in 41 mg/kg NFA group. No increase was observed in *Nrf2*-proficient mice treated with NFT

or NFA at all doses (Fig. 5).

In vivo mutation assay

Results of the *gpt* assay for the kidneys of *Nrf2*-proficient and -deficient mice treated with NFT or NFA are shown in Tables 2, 3 and 4. The *gpt* MFs in *Nrf2*-deficient mice treated with NFT at 70 mg/kg were significantly greater than those in the control group (Table 2). Increases in guanine base substitutions including G:C–T:A or G:C–C:G transversions, were observed in *Nrf2*-deficient mice treated with NFT although there were no statistically significant differences (Table 4). The results of the Spi^- assay are summarized in Table 5. There were no significant changes in the Spi^- MF in *Nrf2*-proficient and -deficient mice treated with NFT or NFA at any dose.

Discussion

Nrf2 plays a crucial role in protection against oxidative stress by transcriptionally upregulating various antioxidant enzymes, including NQO1 (23, 32). Previous studies have shown that *Nrf2*$^{-/-}$ mice show high sensitivity to various toxicants, including the induction of the oxidative stress response following exposure to acetaminophen, 4-vinylcyclohexene diepoxide, pentachlorophenol, 2-amino-3-methylimidazo[4,5-f]quinoline, ferric nitrilotriacetate, and piperonylbutoxide (7, 14, 24, 28, 50, 58, 62). Although there were no dose-dependent effects in either genotype, the mRNA expression level of *Nqo1* in the kidneys of vehicle-treated *Nrf2*$^{-/-}$ mice was significantly lower than that of vehicle-treated *Nrf2*$^{+/+}$ mice, consistent with the results observed for the protein expression of NQO1. Thus, our results confirmed that *Nrf2*$^{-/-}$ mice are susceptible to oxidative stress. NFT administration for 13 weeks resulted in a significant increase in 8-OHdG in a dose-dependent manner, only in the kidneys of *Nrf2*$^{-/-}$ mice. The administration of NFA also tended to result in a dose-dependent increase in 8-OHdG in *Nrf2*$^{-/-}$ mice. These results in the present study suggested that NFT and NFA induced oxidative stress in the kidneys of mice and NFT might induce severer oxidative stress than NFA.

Gpt MFs increased significantly in the kidneys of NFT-treated *Nrf2*$^{-/-}$ mice, but not in *Nrf2*$^{+/+}$ mice. In NFT-treated *Nrf2*$^{-/-}$ mice, the frequencies of specific mutations and, in particular, the rates of G:C–T:A and G:C–C:G transversions increased in a dose-dependent manner. These changes in spectra of *gpt* mutations were consistent with those observed in NFT-treated *gpt* delta rats (27). Since guanine bases are susceptible to

oxidative modification, the characteristics of the mutation spectra suggest that oxidative stress is involved in NFT-induced genotoxicity. Moreover, 8-OHdG causes G:C–T:A transversions via mispairing with adenine in the course of DNA replication (38, 39); accordingly, the formation of 8-OHdG may contribute to the G:C–T:A transversions observed in *Nrf2*$^{-/-}$ mice treated with NFT. Furthermore, NFT failed to induce increases in 8-OHdG in *Nrf2*$^{+/+}$ mice, unlike in rats (27), indicating that the sensitivity to oxidative stress is greater in rats than in mice. Considering that NFT shows carcinogenicity in rats, but not in mice (9), this may explain the difference in NFT carcinogenicity between rats and mice.

Nitro-reduction causes oxidative stress in most nitro compounds, including nitrofurans (2, 3, 4). Nitro-reductase induces a one-electron reduction of the nitro group, yielding nitro anion radicals, and the chemical instability increases various ROS, such as superoxide anions and hydroxyl radicals, via its electron-donating ability (61). ROS generation by nitro-reductase is involved in NFT-induced DNA damage or cytotoxicity in rodent livers and lungs (43, 49). However, our recent report showed that NFA, a constituent compound of NFT with a nitro group, induced a significant increase in the *gpt* MF, without an elevation in 8-OHdG, in *gpt* delta rats (27). In the present study, NFA did not increase MFs of the reporter genes in the kidneys of both genotypes, despite the tendencies of increase in 8-OHdG in NFA-treated *Nrf2*$^{-/-}$ mice. These results about NFA in rats and nice indicated that it is unlikely that oxidative stress is involved in the genotoxicity of NFA; other factors, such as the direct formation of DNA adducts, as observed for other nitrofurans (48, 51), by NFA are likely to contribute to its

genotoxicity.

These results imply that nitro reduction plays a key role in the genotoxicity of NFT. However, our findings indicate the involvement of oxidative DNA damage in genotoxicity in the kidneys of NFT-treated *Nrf2*$^{-/-}$ mice, but not in the kidneys of NFA-treated *Nrf2*$^{-/-}$ mice. Side chain interactions may affect the generation of oxidative stress by nitro-reduction of the nitro group.

The results of the present study demonstrated that oxidative stress is involved in NFT-induced genotoxicity in mouse kidneys, consistent with previous results in rats, and oxidative stress was not involved in the genotoxic mechanism of NFA, a constituent compound of NFT with a nitro group. This might be due to the influence by side chains on the generation of oxidative stress by the nitro-reduction of the nitro group. The oxidative stress induced by side chain binding should be considered in the development of new nitrofuran compounds.

Abstract

Despite its antimicrobial activity, nitrofurantoin (NFT) is a renal carcinogen in rats. Oxidative stress induced by the reduction of the nitro group of NFT may contribute to its genotoxicity. This is supported by our recent results indicating that the structure of the nitrofuran plays a key role in NFT-induced genotoxicity, and oxidative DNA damage is involved in renal carcinogenesis. Nuclear factor erythroid 2-related factor 2 (NRF2) regulates cellular responses to oxidative stress. To clarify the role of oxidative stress in the chemical structure-related genotoxic mechanism of NFT, I performed reporter gene mutation assays for NFT and 5-nitro-2-furaldehyde (NFA) using *Nrf2*-proficient and -deficient *gpt* delta mice. NFT administration for 13 weeks resulted in a significant increase in 8-hydroxydeoxyguanosine (8-OHdG; a marker of oxidative stress) and in the *gpt* mutant frequency, only in the kidneys of *Nrf2*$^{-/-}$ mice. The mutation spectrum, characterized by increased substitutions at guanine bases, suggested that oxidative stress is involved in NFT-induced genotoxicity. However, NFA did not increase the mutation frequency in the kidneys, despite the increased 8-OHdG in NFA-treated *Nrf2*$^{-/-}$ mice. Thus, it is unlikely that oxidative stress is involved in the genotoxic mechanism of NFA. These results imply that nitro reduction plays a key role in the genotoxicity of NFT, but the lack of a role of oxidative stress in the genotoxicity of NFA indicates a potential role of side chain interactions in oxidative stress by nitro-reduction. These findings provide a basis for the development of safe nitrofurans.

NFT

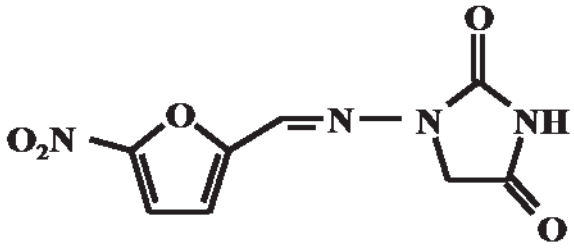

NFA

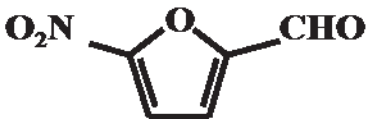

Fig. 1. Chemical structures of NFT and NFA

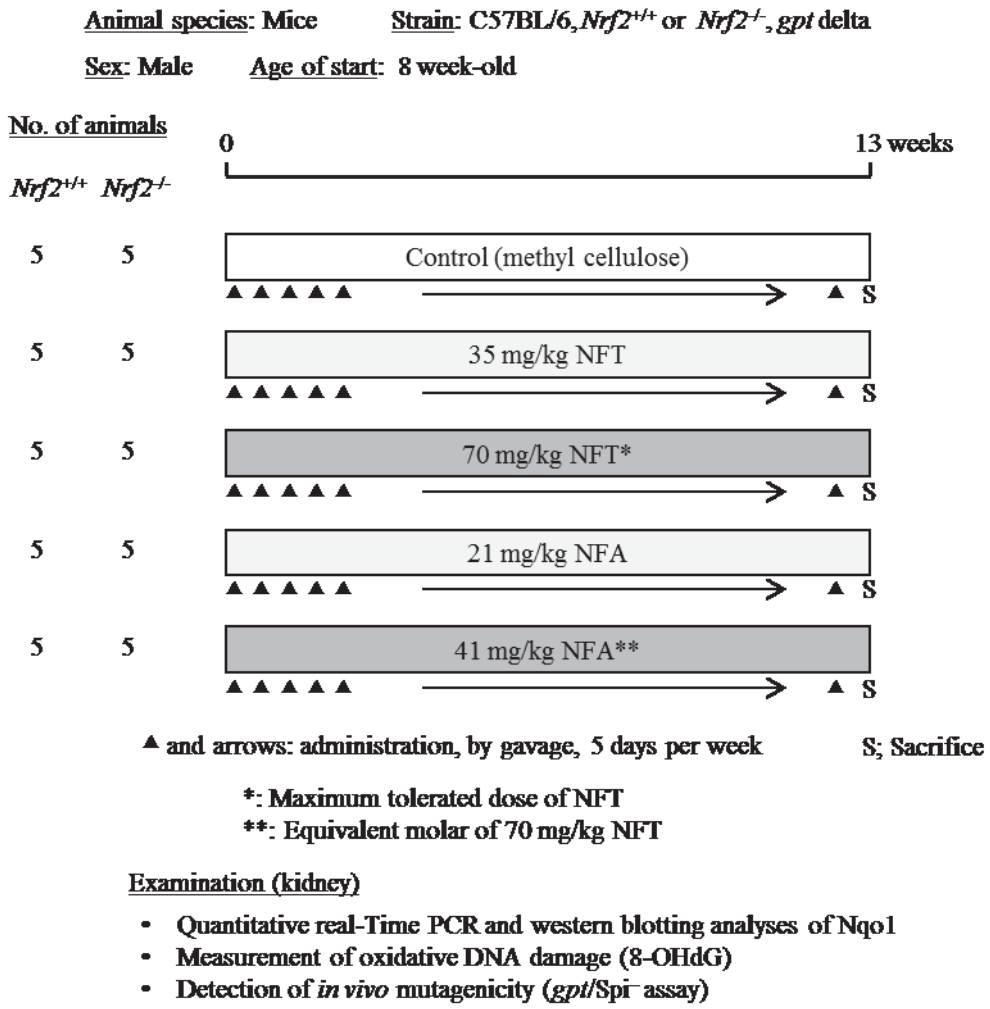

Fig. 2. Experimental design

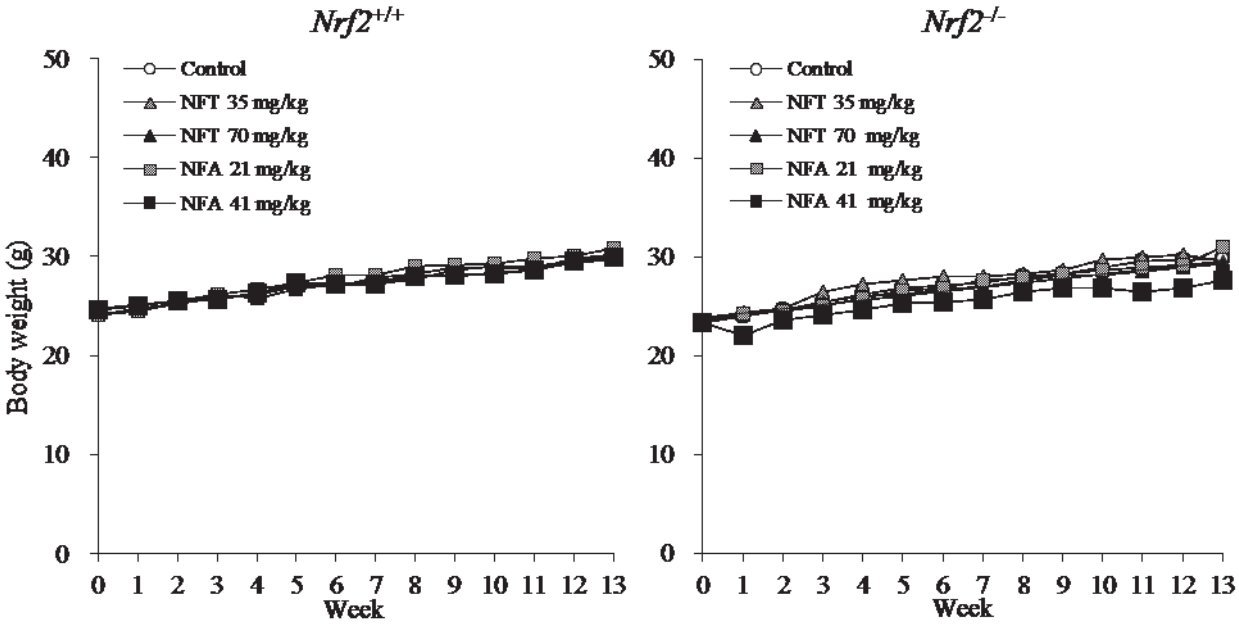

Fig. 3. Growth curves for *Nrf2*$^{+/+}$ (left panel) and *Nrf2*$^{-/-}$ (right panel) mice treated with NFT or NFA for 13 weeks. n=5/group. For both genotypes, there were no significant differences in body weight between treated and untreated mice.

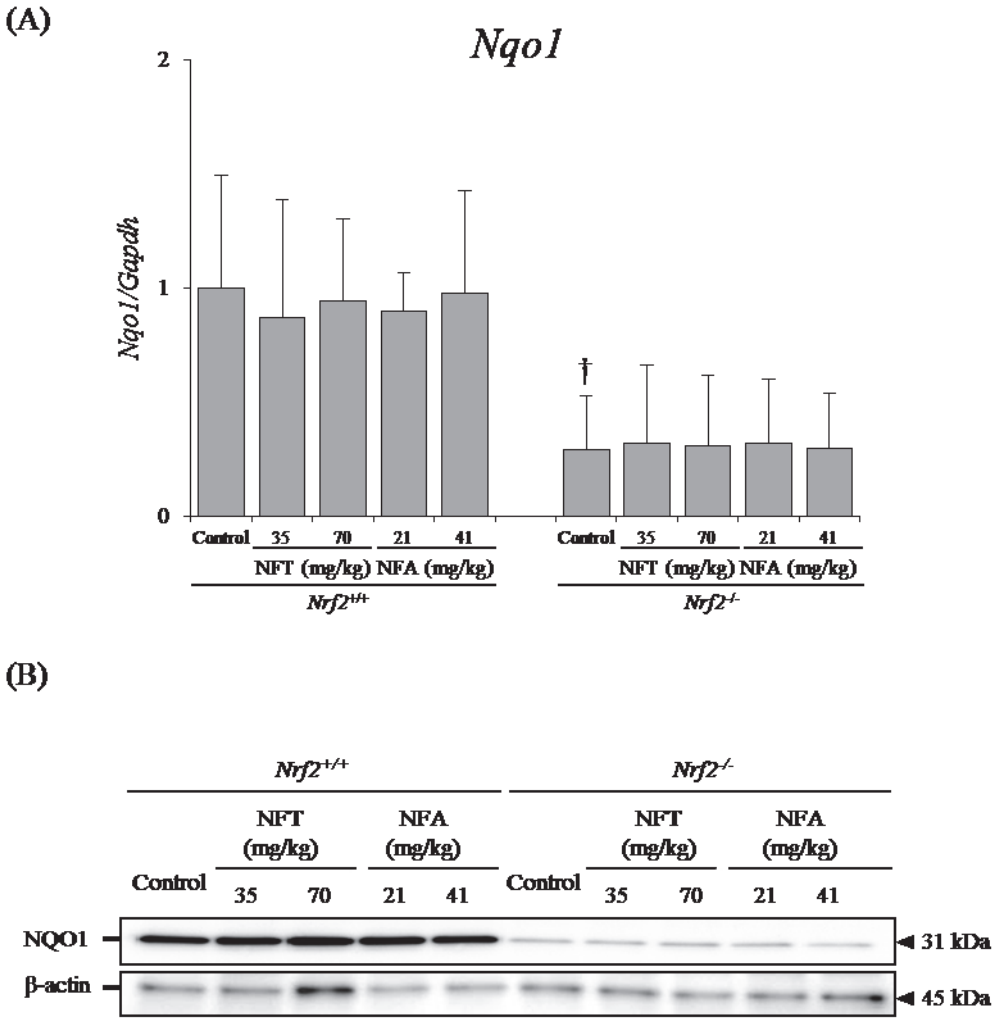

Fig. 4. Changes in the *Nrf2*-target gene *Nqo1* at the mRNA (A) and protein levels (B). (A) Data are presented as means ± SD. n=5/group. †: mRNA expression levels in Nrf2-/- control group were significantly different ($P < 0.05$) from levels in $Nrf2^{+/+}$ control group by Student's *t*-test. (B) Representative image of western blotting about NQO1 and β-actin as an internal control. Homogenized kidneys of 5 mice were used. The expression levels of NQO1 in $Nrf2^{-/-}$ mice are lower than those of $Nrf2^{+/+}$ mice.

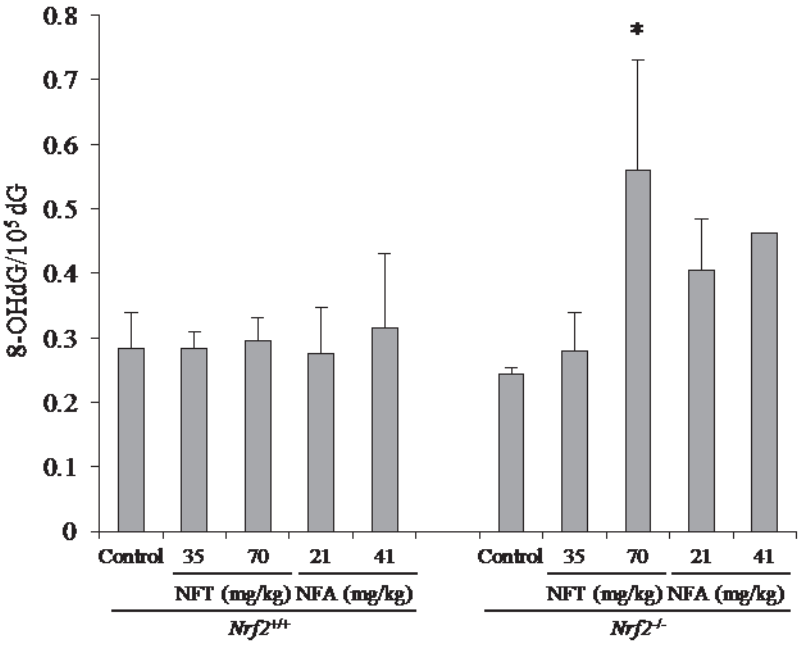

Fig. 5. 8-OHdG levels in the kidneys of *Nrf2*$^{+/+}$ or *Nrf2*$^{-/-}$ *gpt* delta mice treated with NFT or NFA for 13 weeks. Data are presented as means ± SD for 3 mice in the group other than 41 mg/kg NFA. In 41 mg/kg NFA group, the data obtained from one mouse were presented. *: Significantly different ($P < 0.05$) from levels in respective control group by Dunnett's test.

Table 1. Final body and kidney weights of male *Nrf2* $^{+/+}$ or *Nrf2* $^{-/-}$ *gpt* delta mice treated with NFT or NFA for 13 weeks

	Nrf2 $^{+/+}$				
	Control	NFT		NFA	
		35 mg/kg	70 mg/kg	21 mg/kg	41 mg/kg
No. of animals	5	5	5	5	5
Final body weights (g)	30.05 ± 1.51[b]	30.14 ± 1.06	29.62 ± 2.09	30.88 ± 1.25	29.93 ± 2.49
Kidneys (g)	0.39 ± 0.02	0.36 ± 0.01	0.37 ± 0.05	0.37 ± 0.03	0.37 ± 0.05
Kidneys (g%)[a]	1.31 ± 0.07	1.20 ± 0.03	1.25 ± 0.11	1.19 ± 0.09	1.22 ± 0.11

	Nrf2 $^{-/-}$				
	Control	NFT		NFA	
		35 mg/kg	70 mg/kg	21 mg/kg	41 mg/kg
No. of animals	5	5	4	5	5
Final body weights (g)	29.86 ± 2.85	29.60 ± 3.58	29.26 ± 3.15	30.94 ± 2.80	27.59 ± 1.40
Kidneys (g)	0.36 ± 0.04	0.36 ± 0.08	0.38 ± 0.06	0.36 ± 0.05	0.31 ± 0.05
Kidneys (g%)[a]	1.20 ± 0.04	1.22 ± 0.17	1.28 ± 0.10	1.15 ± 0.07	1.13 ± 0.16

[a] Kidneys-to-body weight ratios (relative weights) are given as g organ weight/g body weight.

[b] Means ± SD.

Table 2. *Gpt* mutation frequencies in kidneys of *Nrf2* $^{+/+}$ or *Nrf2* $^{-/-}$ *gpt* delta mice treated with NFT or NFA for 13 weeks

Genotype	Treatment	Animal No.	Cm^R colonies ($\times 10^5$)	6-TG^R and Cm^R colonies	MF ($\times 10^{-5}$)	Mean ± SD
Nrf2 $^{+/+}$	Control	W1	25.02	7	0.28	
		W2	18.00	10	0.56	
		W3	18.09	10	0.55	
		W4	8.24	5	0.61	
		W5	36.99	11	0.30	0.46 ± 0.16
	NFT 35 mg/kg	W7	13.95	9	0.65	
		W8	23.09	7	0.30	
		W9	25.11	15	0.60	
		W10	12.33	5	0.41	
		W11	15.12	10	0.66	0.52 ± 0.16
	NFT 70 mg/kg	W13	20.61	4	0.19	
		W14	22.14	11	0.50	
		W15	17.64	12	0.68	
		W16	7.25	5	0.69	0.52 ± 0.23
	NFA 21 mg/kg	W19	22.91	10	0.44	
		W20	11.61	5	0.43	
		W21	32.49	6	0.18	
		W22	19.80	7	0.35	
		W23	15.44	4	0.26	0.33 ± 0.11
	NFA 41 mg/kg	W25	35.15	3	0.09	
		W26	24.57	6	0.24	
		W27	41.09	3	0.07	
		W28	7.74	4	0.52	
		W29	16.02	10	0.62	0.31 ± 0.25
Nrf2 $^{-/-}$	Control	Ho1	8.15	4	0.49	
		Ho2	24.93	8	0.32	
		Ho3	20.43	5	0.24	
		Ho4	11.43	2	0.17	
		Ho5	21.87	12	0.55	0.36 ± 0.16
	NFT 35 mg/kg	Ho7	12.15	3	0.25	
		Ho8	10.26	1	0.10	
		Ho9	28.80	11	0.38	
		Ho10	24.71	16	0.65	
		Ho11	20.34	10	0.49	0.37 ± 0.21
	NFT 70 mg/kg	Ho15	10.22	8	0.78	
		Ho16	10.22	10	0.98	
		Ho17	19.40	18	0.93	
		Ho18	18.23	13	0.71	0.85 ± 0.12*
	NFA 21 mg/kg	Ho19	11.48	2	0.17	
		Ho20	16.56	8	0.48	
		Ho22	18.77	24	1.28	
		Ho23	11.16	3	0.27	
		Ho24	19.67	5	0.25	0.49 ± 0.45
	NFA 41 mg/kg	Ho25	16.74	4	0.24	
		Ho26	11.16	7	0.63	
		Ho28	4.10	1	0.24	
		Ho29	14.99	7	0.47	
		Ho30	18.14	13	0.72	0.46 ± 0.22

* $P < 0.05$ vs. respective control group

Cm^R, chloramphenicol resistant; 6-TG^R, 6-thioguanine resistant; MF, mutant frequensy

Table 3. Mutation spectra in the kidneys of *Nrf2* $^{+/+}$ *gpt* delta mice treated with NFT or NFA for 13 weeks

	Control		NFT 35 mg/kg		NFT 70 mg/kg		NFA 21 mg/kg		NFA 41 mg/kg	
	Number (%)	Specific MFs (10^{-5})	Number (%)	Specific MFs (10^{-5})	Number (%)	Specific MFs (10^{-5})	Number (%)	Specific MFs (10^{-5})	Number (%)	Specific MFs (10^{-5})
Base substitution										
Transversions										
G:C-T:A	8 (26.7)	0.10 ± 0.08	11 (28.9)	0.11 ± 0.09	3 (12.0)	0.07 ± 0.12	5 (18.5)	0.05 ± 0.06	8 (33.3)	0.10 ± 0.10
G:C-C:G	0	0	2 (5.3)	0.02 ± 0.03	3 (12.0)	0.05 ± 0.06	0	0	2 (8.3)	0.03 ± 0.06
A:T-T:A	0	0	2 (5.3)	0.03 ± 0.06	0	0	2 (7.4)	0.02 ± 0.03	1 (4.2)	0.03 ± 0.06
A:T-C:G	0	0	0	0	3 (12.0)	0.05 ± 0.06**	1 (3.7)	0.01 ± 0.02	0	0
Transisions										
G:C-A:T	8 (26.7)	0.09 ± 0.05	13 (34.2)	0.15 ± 0.12	7 (28.0)	0.07 ± 0.10	13 (48.1)	0.13 ± 0.03	4 (16.7)	0.04 ± 0.08
A:T-G:C	5 (16.7)	0.06 ± 0.05	3 (7.9)	0.04 ± 0.06	0	0	0	0	1 (4.2)	0.01 ± 0.02
Deletion										
Single bp	2 (6.7)	0.05 ± 0.11	0	0	3 (12.0)	0.03 ± 0.03	4 (14.8)	0.05 ± 0.03	3 (12.5)	0.03 ± 0.03
Over 2 bp	3 (10)	0.02 ± 0.05	7 (18.4)	0.08 ± 0.05	0	0	1 (3.7)	0.02 ± 0.04	3 (12.5)	0.03 ± 0.03
Insertion	2 (6.7)	0.01 ± 0.02	0	0	3 (12.0)	0.05 ± 0.06	0	0	2 (8.3)	0.02 ± 0.06
Complex	2 (6.7)	0.02 ± 0.05	0	0	3 (12.0)	0.03 ± 0.04	1 (3.7)	0.01 ± 0.02	0	0
Total	30	0.35	38	0.43	25	0.34	27	0.28	24	0.29

** $P < 0.01$, vs. control group

MF, mutant frequency

Table 4. Mutation spectra in the kidneys of *Nrf2*$^{-/-}$ *gpt* delta mice treated with NFT or NFA for 13 weeks

	Control		NFT 35 mg/kg		NFT 70 mg/kg		NFA 21 mg/kg		NFA 41 mg/kg	
	Number (%)	Specific MFs (10^{-5})	Number (%)	Specific MFs (10^{-5})	Number (%)	Specific MFs (10^{-5})	Number (%)	Specific MFs (10^{-5})	Number (%)	Specific MFs (10^{-5})
Base substitution										
Transversions										
G:C-T:A	4 (13.8)	0.06 ± 0.06	8 (22.2)	0.08 ± 0.06	9 (21.4)	0.15 ± 0.13	7 (31.8)	0.08 ± 0.05	3 (9.4)	0.05 ± 0.08
G:C-C:G	2 (6.9)	0.02 ± 0.03	3 (8.3)	0.02 ± 0.04	7 (16.7)	0.13 ± 0.13	2 (9.1)	0.03 ± 0.04	4 (12.5)	0.06 ± 0.07
A:T-T:A	0	0	0	0	1 (2.4)	0.02 ± 0.05	1 (4.5)	0.01 ± 0.03	2 (6.3)	0.02 ± 0.05
A:T-C:G	2 (6.9)	0.02 ± 0.04	1 (2.8)	0.01 ± 0.02	0	0	0	0	0	0
Transisions										
G:C-A:T	14 (48.3)	0.15 ± 0.08	15 (41.7)	0.14 ± 0.06	13 (31.0)	0.22 ± 0.09	6 (27.3)	0.07 ± 0.05	12 (37.5)	0.14 ± 0.17
A:T-G:C	0	0	2 (5.6)	0.02 ± 0.02	1 (2.4)	0.02 ± 0.05	1 (4.5)	0.01 ± 0.02	1 (3.1)	0.02 ± 0.04
Deletion										
Single bp	6 (20.7)	0.07 ± 0.05	3 (8.3)	0.02 ± 0.03	5 (11.9)	0.09 ± 0.07	2 (9.1)	0.03 ± 0.04	1 (3.1)	0.01 ± 0.03
Over 2 bp	1 (3)	0.01 ± 0.02	2 (5.6)	0.02 ± 0.02	2 (4.8)	0.03 ± 0.05	0	0	4 (12.5)	0.05 ± 0.05
Insertion	0	0	1 (2.8)	0.01 ± 0.02	1 (2.4)	0.02 ± 0.05	1 (4.5)	0.02 ± 0.04	2 (6.3)	0.06 ± 0.11
Complex	0	0	1 (2.8)	0.01 ± 0.02	3 (7.1)	0.06 ± 0.09	2 (9.1)	0.02 ± 0.05	3 (9.4)	0.05 ± 0.08
Total	29	0.32	36	0.33	42	0.75	22	0.28	32	0.46

MF, mutant frequency

Table 5. Spi⁻ mutant frequencies in kidneys of *Nrf2* $^{+/+}$ or *Nrf2* $^{-/-}$ *gpt* delta mice treated with NFT or NFA for 13 weeks

Genotype	Treatment	Animal No.	Plaques within XL-1 Blue MRA ($\times 10^5$)	Plaques within XL-1 Blue MRA (P2)	MF ($\times 10^{-5}$)	Mean ± SD
Nrf2 $^{+/+}$	Control	W1	20.34	4	0.20	
		W2	18.45	2	0.11	
		W3	11.70	3	0.26	
		W4	4.23	4	0.95	
		W5	33.39	8	0.24	0.35 ± 0.34
	NFT 35 mg/kg	W7	22.23	11	0.49	
		W8	10.35	6	0.58	
		W9	19.71	12	0.61	
		W10	7.29	5	0.69	
		W11	13.95	2	0.14	0.50 ± 0.21
	NFT 70 mg/kg	W13	19.35	5	0.26	
		W14	15.39	12	0.78	
		W15	22.77	4	0.18	
		W16	4.41	2	0.45	
		W17	4.95	0	0.00	0.33 ± 0.30
	NFA 21 mg/kg	W19	26.46	7	0.26	
		W20	10.98	4	0.36	
		W21	25.20	8	0.32	
		W22	16.74	7	0.42	
		W23	10.89	4	0.37	0.35 ± 0.06
	NFA 41 mg/kg	W25	36.09	4	0.11	
		W26	16.74	7	0.42	
		W27	34.56	15	0.43	
		W28	10.44	4	0.38	
		W29	13.32	5	0.38	0.34 ± 0.13
Nrf2 $^{-/-}$	Control	Ho1	6.39	3	0.47	
		Ho2	19.62	5	0.25	
		Ho3	14.04	2	0.14	
		Ho4	10.53	6	0.57	
		Ho5	20.34	5	0.25	0.34 ± 0.18
	NFT 35 mg/kg	Ho7	13.14	7	0.53	
		Ho8	10.44	2	0.19	
		Ho9	26.01	7	0.27	
		Ho10	21.78	13	0.60	
		Ho11	21.69	12	0.55	0.43 ± 0.18
	NFT 70 mg/kg	Ho15	12.69	7	0.55	
		Ho16	12.24	5	0.41	
		Ho17	18.54	9	0.49	
		Ho18	19.62	7	0.36	0.45 ± 0.09
	NFA 21 mg/kg	Ho19	11.34	0	0.00	
		Ho20	13.86	5	0.36	
		Ho22	36.72	12	0.33	
		Ho23	14.13	4	0.28	
		Ho24	15.66	12	0.77	0.35 ± 0.27
	NFA 41 mg/kg	Ho25	17.64	8	0.45	
		Ho26	9.27	3	0.32	
		Ho28	3.69	3	0.81	
		Ho29	14.04	7	0.50	
		Ho30	23.58	9	0.38	0.49 ± 0.19

MF, mutant frequency

Chapter 2

Mechanisms of oxidative stress-induced *in vivo* mutagenicity by potassium bromate and nitrofurantoin

Introduction

The formation of reactive oxygen species (ROS) is considered one of the key factors in chemical carcinogenesis. However, the actual role of oxidative stress remains unclear. Some reports suggest that ROS play an important role in the promotion of chemical carcinogenesis by stimulating the proliferation of initiated cells (29, 37, 44), while others demonstrate that ROS might be an initiator by forming oxidized DNA lesions (37, 42, 45, 57). 8-hydroxydeoxyguanosine (8-OHdG) is the most abundant oxidized DNA lesion among the many oxidized nucleosides known and is fairly stable (25). The repair of 8-OHdG is carried out by the base excision repair enzymes. In humans, OGG1, MUTYH, and MTH1 repair 8-OHdG and contribute to the protection of genomic DNA from oxidative stress (35). The remaining 8-OHdG is considered to cause G:C–T:A transversions by mispairing with adenine and 8-OHdG (38, 39).

Potassium bromate ($KBrO_3$) induces renal cell tumor formation in F344 rats and has been classified as a genotoxic carcinogen because of positive mutagenicity in the Ames (21), chromosome aberration (20), and micronucleus tests (13). The studies demonstrating the induction of 8-OHdG by $KBrO_3$ *in vitro* and *in vivo* suggest that 8-OHdG plays a key role in $KBrO_3$ mutagenesis and carcinogenesis (1, 26, 56, 59). It was reported that $KBrO_3$ produces bromine radicals, which oxidize guanine bases (36). Additionally, our previous study using the two-stage rat renal carcinogenesis model clarified the *in vivo* mutagenicity and initiation following oxidized DNA lesion in the kidneys of rats administered $KBrO_3$ (55) and showed that high amounts of 8-OHdG resulted in several types of mutations, including deletion mutations, in addition to

G:C–T:A transversions (55). The antimicrobial compound nitrofurantoin (NFT) is also known as a renal carcinogen in rats and is prohibited for veterinary use in Japan (18). The reduction of the nitro group of NFT induces oxidative stress, which exerts antibacterial activity (2, 3, 4). Moreover, the involvement of oxidative stress is suspected in NFT-induced carcinogenesis. In fact, our recent study showed increased levels of 8-OHdG and *gpt* mutant frequencies (MFs) with guanine base substitution mutations, including G:C–T:A transversions, in the kidneys of *gpt* delta rats treated with NFT (27). Nonetheless, the relationship between the formation of 8-OHdG and several types of mutations, including deletion mutations and G:C–T:A transversions, remains unclear.

One of the redox-sensitive transcription factors, nuclear factor erythroid 2-related factor 2 (NRF2), regulates cellular responses to oxidative stress by transactivation of antioxidant response element (ARE)-bearing genes encoding antioxidant related enzymes, such as NAD(P)H:quinone oxidoreductase 1 (NQO1), heme oxygenase 1 (HO1), and glutathione S-transferase (GST) (23, 32). Because of the function of NRF2, *Nrf2*-deficient mice show higher sensitivity to various toxicants that induce oxidative stress (7, 14, 24, 28, 50, 58, 62); therefore, these mice are quite suitable for investigation of the involvement of oxidative stress in chemical-induced genotoxicity and carcinogenesis.

In the present study, 4- and 13-week exposure of *Nrf2*-proficient and -deficient mice to $KBrO_3$ in drinking water or NFT in diet followed by reporter gene mutation assays (34, 40) and measurement of 8-OHdG levels in the kidney DNA was performed

to clarify the relationship between the formation of 8-OHdG and several types of mutations. In addition, this study aimed to elucidate the detailed mechanism of oxidative stress involvement in $KBrO_3$- or NFT-induced renal carcinogenesis.

Materials and Methods

Chemicals

Potassium bromate ($KBrO_3$, MW 167, CAS No. 7758-01-2) and NFT ($C_8H_6N_4O_5$, MW 238.2, CAS No. 67-20-9) were purchased from Wako Pure Chemical Industries (Osaka, Japan) and Sigma-Aldrich (St. Louis, MO, USA), respectively.

Animals, diet, and housing conditions

The study protocol was approved by the Animal Care and Utilization Committee of the National Institute of Health Sciences. *Nrf2*-deficient mice with C57BL/6J background established by Itoh *et al*. (22) were crossed with *gpt* delta mice with C57BL/6J background (Japan SLC, Shizuoka, Japan). *Nrf2*$^{-/-}$ *gpt* delta mice and *Nrf2*$^{+/+}$ *gpt* delta mice were then obtained from the F1 generation and genotyped by polymerase chain reaction (PCR) with DNA taken from the tail of each mouse. All mice were housed in polycarbonate cages (3 to 5 mice per cage) with hardwood chips for bedding in a conventional animal facility maintained at a controlled temperature (23±2°C) and humidity (55%±5%), with 12 air changes per hour and a 12-h light/dark cycle. Mice were given free access to CRF-1 basal diet (Charles River Japan, Kanagawa, Japan) and tap water.

Experimental design

Experimental design is described in Fig. 6. Six-week-old male mice of each genotype were divided into six groups (four to eight mice per group). $KBrO_3$ was

dissolved in distilled water at concentration of 1,500 ppm, and the prepared water was given to the animals *ad libitum* for 4 or 13 weeks. NFT was mixed in CRF-1 basal diet at concentration of 2,500 ppm, and the prepared diet was given to the animals *ad libitum* for 4 or 13 weeks. Mice of the control group were given distilled water and CRF-1 basal diet. Dose levels of $KBrO_3$ and NFT were selected as each maximum dose that could be administrated to mice for 13 weeks based on the report of intestinal carcinogenesis in *Nrf2*$^{-/-}$ mice (62), a subacute toxicity study of $KBrO_3$ (30), and toxicology and carcinogenesis study of NFT conducted by the National Toxicology Program (9). In the present study, the groups of 4- and 13-week administration were set for the objective of detection of early changes and subsequent changes in 8-OHdG levels and *in vivo* mutagenicity induced by $KBrO_3$ or NFT, respectively. Body weights were measured every week. The kidneys-to-body weight ratios (relative weights) were calculated as g organ weight/g body weight. Animals were killed by exsanguination under isoflurane (Mylan Inc., Tokyo, Japan) anesthesia, and at necropsy, the bilateral kidneys were collected, and their weights were measured. A portion of the kidney tissues was frozen with liquid nitrogen and stored at -80°C for use in the *in vivo* mutation assay and 8-OHdG measurement. Another portion was homogenized in ISOGEN (Nippon Gene, Tokyo, Japan) and stored at -80°C until used for isolation of total RNA.

RNA isolation and quantitative real-time PCR for evaluation of mRNA expression

Total RNA was extracted using ISOGEN according to the manufacturer's instructions. cDNA of total RNA was obtained using a High-Capacity cDNA Reverse

Transcription Kit (Life Technologies).

All PCR reactions were performed with the Applied Biosystems 7900HT FAST Real-Time PCR System with primers for mouse *Nqo1* (coding NAD(P)H:quinone oxidoreductase 1) obtained from TaqMan® Gene Expression Assays and TaqMan® Rodent GAPDH Control Reagents. The expression levels of the target gene were calculated by the relative standard curve method and were determined as ratios to *Gapdh* levels. Data are presented as fold-change values of treated samples relative to controls.

Measurement of 8-OHdG

Three animals in each group were selected randomly, and kidneys of those animals were used for the measurement of 8-OHdG. Renal DNA of *Nrf2*$^{-/-}$ *gpt* delta mice and *Nrf2*$^{+/+}$ *gpt* delta mice was extracted and digested as described previously (54). Briefly, nuclear DNA was extracted with a DNA Extractor WB Kit (Wako Pure Chemical Co.). For further prevention of artifactual oxidation in the cell lysis step, deferoxamine mesylate (Sigma-Aldrich) was added to the lysis buffer. The DNA was digested to deoxynucleotides by treatment with nuclease P1 and alkaline phosphatase, using the 8-OHdG Assay Preparation Reagent Set (Wako Pure Chemical Co.). The levels of 8-OHdG (8-OHdG/10^5 dG) were measured by high-performance liquid chromatography with an electrochemical detection system (Coulochem II; ESA, Bedford, MA, USA) as previously reported (55).

In vivo mutation assays

6-Thioguanine (6-TG) and Spi$^-$ selections were performed using the methods described by Nohmi *et al.* (40). Briefly, genomic DNA was extracted from the kidneys of animals in each group using the RecoverEase DNA isolation kit (Agilent Technologies, Santa Clara, CA, USA), and lambda EG10 DNA (48 kb) was rescued as phages by *in vitro* packaging using Transpack packaging extract (Agilent Technologies). For 6-TG selection, packaged phages were incubated with *Escherichia coli* YG6020, which expresses Cre recombinase, and converted to plasmids carrying genes encoding glutamic–pyruvate transaminase and chloramphenicol acetyltransferase. Infected cells were mixed with molten soft agar and poured onto agar plates containing chloramphenicol and 6-TG. In order to determine the total number of rescued plasmids, infected cells were also poured on plates containing chloramphenicol without 6-TG. The plates were then incubated at 37°C for selection of 6-TG-resistant colonies, and *gpt* MF was calculated by dividing the number of *gpt* mutants after clonal correction by the number of rescued phages. *Gpt* mutations were characterized by amplifying a 739-bp DNA fragment containing the 456-bp coding region of the *gpt* gene (40) and sequencing the PCR products with an Applied Biosystems 3730*xl* DNA Analyzer (Life Technologies, Carlsbad, CA, USA). For Spi$^-$ selection, packaged phages were incubated with *E. coli* XL-1 Blue MRA for survival titration and *E. coli* XL-1 Blue MRA P2 for mutant selection. Infected cells were mixed with molten lambda-trypticase agar and poured onto lambda-trypticase agar plates. The next day, plaques (Spi$^-$ candidates) were punched out with sterilized glass pipettes, and the agar plugs were suspended in SM

buffer. The Spi$^-$ phenotype was confirmed by spotting the suspensions on three types of plates on which XL-1 Blue MRA, XL-1 Blue MRA P2, or WL95 P2 strain was spread with soft agar. Spi$^-$ mutants, which manifested as clear plaques, were counted on every plate.

Statistical analysis

The significance of differences in the results for body weight, kidney weight, mRNA expression levels, 8-OHdG levels, *gpt* and Spi$^-$ MFs, and *gpt*- and Spi$^-$-mutation spectra were analyzed by Student's *t*-test depending on the homogeneity. P values < 0.05 were considered significant.

Results

Body and kidney weights

Body and kidney weights of *Nrf2*-proficient and -deficient mice treated with $KBrO_3$ or NFT for 4 or 13 weeks are summarized in Fig. 7 and Table 6. For both genotypes and time points, no significant change was observed in body and kidney weights of treated and respective control animals.

Quantitative real-time PCR for evaluation of Nqo1 *mRNA expression*

Expression levels of *Nqo1* in the kidneys are shown in Fig. 8. In $Nrf2^{+/+}$ mice, the expression level of *Nqo1* was significantly increased by 4- or 13-week exposure to $KBrO_3$ ($P < 0.01$) and 13-week exposure to NFT ($P < 0.05$) when compared with the control group. Four-week exposure to NFT resulted in the tendencies of increased expression of *Nqo1* in $Nrf2^{+/+}$ mice. In $Nrf2^{-/-}$ mice, increased *Nqo1* expression was not induced by $KBrO_3$ or NFT treatment at either time point. The *Nqo1* expression levels of control, $KBrO_3$-treated, and NFT-treated $Nrf2^{-/-}$ mice were significantly lower ($P < 0.01$) than those of the corresponding $Nrf2^{+/+}$ mice at both time points.

Measurement of 8-OHdG in kidney DNA

The results of 8-OHdG measurement in the kidneys are shown in Fig. 9. At both time points, $KBrO_3$ treatment significantly increased the level of 8-OHdG in the kidneys of both genotypes, and the degree of 8-OHdG increase was as follows: 4-week $Nrf2^{+/+}$, × 2.8; 4-week $Nrf2^{-/-}$, × 3.6; 13-week $Nrf2^{+/+}$, × 2.1; 13-week $Nrf2^{-/-}$, × 3.3, vs.

respective control). On the other hand, NFT treatment did not increase the level of 8-OHdG in the kidneys of either genotype at either time point. Between the *Nrf2*-proficient and -deficient mice of each treatment group, the 8-OHdG level was not significantly changed.

In vivo mutation assay of kidneys

The results of the *gpt* assay of the kidneys of *Nrf2*-proficient and -deficient mice treated with $KBrO_3$ or NFT are shown in Tables 7 to 12. At both of 4- and 13-week, $KBrO_3$-treated mice showed significant increase or tendencies of increase of *gpt* MFs compared with those in the respective control groups (Tables 7 and 8). The degree of increase of *gpt* MFs by 13-week treatment with $KBrO_3$ was as follows: $Nrf2^{+/+}$, × 2.2; $Nrf2^{-/-}$, × 4.4, vs. respective control (Table 8). Specific MFs of deletion mutations were increased in the spectrum analysis of *gpt* mutants in $KBrO_3$-treated mice (Tables 10 and 11). The frequencies of deletion mutations of more than two base pairs were increased by 13-week treatment with $KBrO_3$ in both genotypes (Table 11).

Furthermore, in both genotypes, *gpt* MFs were increased by 13-week treatment with NFT, despite no change at 4 weeks (Tables 7 and 9). The degree of increase of *gpt* MFs by 13-week treatment with NFT was as follows: $Nrf2^{+/+}$, × 2.1; $Nrf2^{-/-}$, × 3.3, vs. respective control (Table 9). In both genotypes, guanine base substitution mutations, including G:C–T:A or G:C–C:G transversion mutations, were increased by 13-week treatment with NFT (Table 12).

The results of the Spi^- assay of the kidneys of *Nrf2*-proficient and -deficient

mice treated with $KBrO_3$ or NFT are shown in Tables 13 to 16. At both time points, $KBrO_3$-treated mice showed significant increase or the tendencies of increase of Spi^- MFs compared with those in the respective control groups (Tables 13 and 14). The degree of increase of Spi^- MFs by 13-week treatment with $KBrO_3$ was as follows: *Nrf2*$^{+/+}$, × 3.0; *Nrf2*$^{-/-}$, × 4.1; vs. respective control (Table 14). In the spectrum analysis of Spi^- mutants in $KBrO_3$-treated mice, specific MFs of deletion mutations were increased (Tables 15 and 16), consistent with that of *gpt* mutants. In both genotypes and at both time points, NFT treatment did not change Spi^- MFs (Tables 13 and 14).

Discussion

It is well known that transcriptional upregulation of various antioxidant enzymes, including NQO1 and HO1, is regulated by NRF2, which protect cells from oxidative stress (23, 32). In several studies, *Nrf2*$^{-/-}$ mice showed higher sensitivity to various toxicants that induced oxidative stress (7, 14, 24, 28, 50, 58, 62). In fact, the mRNA expression level of *Nqo1* in the kidneys of vehicle-treated *Nrf2*$^{-/-}$ mice was significantly lower than that of vehicle-treated *Nrf2*$^{+/+}$ mice, and there was no elevation of the level in $KBrO_3$- or NFT-treated *Nrf2*$^{-/-}$ mice despite the elevation in *Nrf2*$^{+/+}$ mice. Thus, in the present study, *Nrf2*$^{-/-}$ mice were confirmed to be susceptible to oxidative stress. As previously reported, using this highly oxidative stress-sensitive animal gives us important knowledge about the involvement of oxidative stress in chemical-induced genotoxicity and carcinogenesis (7, 14, 24, 28, 50, 58, 62).

Four or thirteen-week administration of 1,500 ppm $KBrO_3$ in drinking water significantly increased the level of 8-OHdG in the kidneys of both genotypes. At both time points, the degree of 8-OHdG increase was higher in *Nrf2*$^{-/-}$ mice than in *Nrf2*$^{+/+}$ mice. Meanwhile, increases of *gpt* and Spi$^-$ MFs were detected, and the tendencies of the degree of increase of *gpt* and Spi$^-$ MFs at 13-week exposure were the same as those of 8-OHdG. In the spectrum analysis of *gpt* and Spi$^-$ mutants in $KBrO_3$-treated *Nrf2*$^{-/-}$ mice, specific MFs of deletion mutations were increased, consistent with a previous study of rats (27), accompanied with the increase of the frequencies of deletion mutations of more than two base pairs. An *in vitro* report demonstrated that error in the repair process of 8-OHdG induced by $KBrO_3$ treatment caused double-strand breaks

(DSBs) in human cells, and DSBs resulted in a large deletion (33). Considering these mechanisms, the increase in size of deletion mutations might reflect the accumulation of high amounts of 8-OHdG in the nuclei due to $KBrO_3$. These results suggested that the formation of 8-OHdG induced by oxidative stress was directly involved in the increase of deletion mutations in $KBrO_3$-treated animals. It was suspected that the formation of high amounts of 8-OHdG owing to the strong potential of $KBrO_3$ as an oxidizing agent might exceed the repairing capacity of base excision repair enzymes.

Four or thirteen-week administration of 2,500 ppm NFT in diet did not increase the level of 8-OHdG in the kidneys of either genotype. In the previous study, the level of 8-OHdG was increased in the kidneys of *Nrf2*$^{-/-}$ mice by oral administration of NFT at 70 mg/kg (52). Lower exposure levels of NFT in the present study compared with those of the previous study did not induce the elevation of 8-OHdG levels. On the other hand, 13-week administration of 2,500 ppm NFT in diet significantly increased *gpt* MFs with guanine base substitution mutations in the kidneys of both genotypes. The degree of increase of *gpt* MFs was higher in *Nrf2*$^{-/-}$ mice than in *Nrf2*$^{+/+}$ mice. These results implied that the vulnerability to oxidative stress caused by the deficiency of *Nrf2* leads to more mutations in NFT-treated mice. Thus, in the genotoxic mechanism of NFT, the formation of 8-OHdG induced by oxidative stress might not be involved in the increase of guanine base substitution mutations. Considering our previous studies, which suggested the involvement of oxidative stress in the chemical structure-related genotoxic mechanism of NFT in rodents (27, 52), further studies are requested to identify oxidative stress markers other than 8-OHdG which might be crucial to the

genotoxicity of NFT, though the present study did not identify them.

In recent years, the level of 8-OHdG has been frequently used as a marker of oxidative stress in human diseases (5, 19). In addition, some reports demonstrated the involvement of oxidative stress in chemical-induced genotoxicity and carcinogenesis using the increase of 8-OHdG level as a parameter of oxidative stress in experimental animals (7, 14, 24, 28, 50, 58, 62). However, the relationship between the formation of 8-OHdG and subsequent mutations, including deletion mutations and G:C–T:A transversions, had not been clarified. The revelation of the relationship between 8-OHdG and several types of mutations induced by $KBrO_3$ or NFT provides new insight into oxidative stress-related *in vivo* mutagenicity.

The present study demonstrated that the formation of 8-OHdG, which resulted from the oxidizing potential of $KBrO_3$, was directly involved in the increase of deletion mutations; however, oxidative stress-related factors other than 8-OHdG might play a critical role in NFT-induced guanine base substitution mutations. This was the first study to investigate the relationship between 8-OHdG and several types of mutations caused by oxidative stress-inducing chemicals. The accumulation of these detailed examinations such as further research on 8-OHdG about individual chemical substance leads to accurate risk assessment of oxidative stress in carcinogenicity.

Abstract

Oxidative stress is well known as a key factor of chemical carcinogenesis. However, the actual role of oxidative stress in carcinogenesis such as oxidative stress-related *in vivo* mutagenicity remains unclear. It has been reported that 8-hydroxydeoxyguanosine (8-OHdG), an oxidized DNA lesion, might contribute to chemical carcinogenesis. Potassium bromate ($KBrO_3$) and nitrofurantoin (NFT) are known as renal carcinogens in rats. Our previous studies showed an increase of mutant frequencies accompanied with an increased level of 8-OHdG in the kidneys of rodents following $KBrO_3$ or NFT exposure. Furthermore, $KBrO_3$ and NFT induced different types of gene mutations. Thus, in the present study, I performed reporter gene mutation assays and 8-OHdG measurements following $KBrO_3$ or NFT exposure using *Nrf2*-proficient and -deficient mice to clarify the relationship between $KBrO_3$- or NFT-induced oxidative stress and subsequent genotoxicity. The administration of 1,500 ppm of $KBrO_3$ in drinking water resulted in the increase of deletion mutations accompanied with the increase of 8-OHdG level, and the administration of 2,500 ppm of NFT in diet induced the increase of guanine base substitution mutations without elevation of 8-OHdG level in *Nrf2*-deficient mice. These results demonstrated that the formation of 8-OHdG, which resulted from the oxidizing potential of $KBrO_3$, was directly involved in the increase of deletion mutations, although factors concerning oxidative stress other than 8-OHdG might be crucial for NFT-induced guanine base substitution mutations. The present study provides new insight into oxidative stress-related *in vivo* mutagenicity.

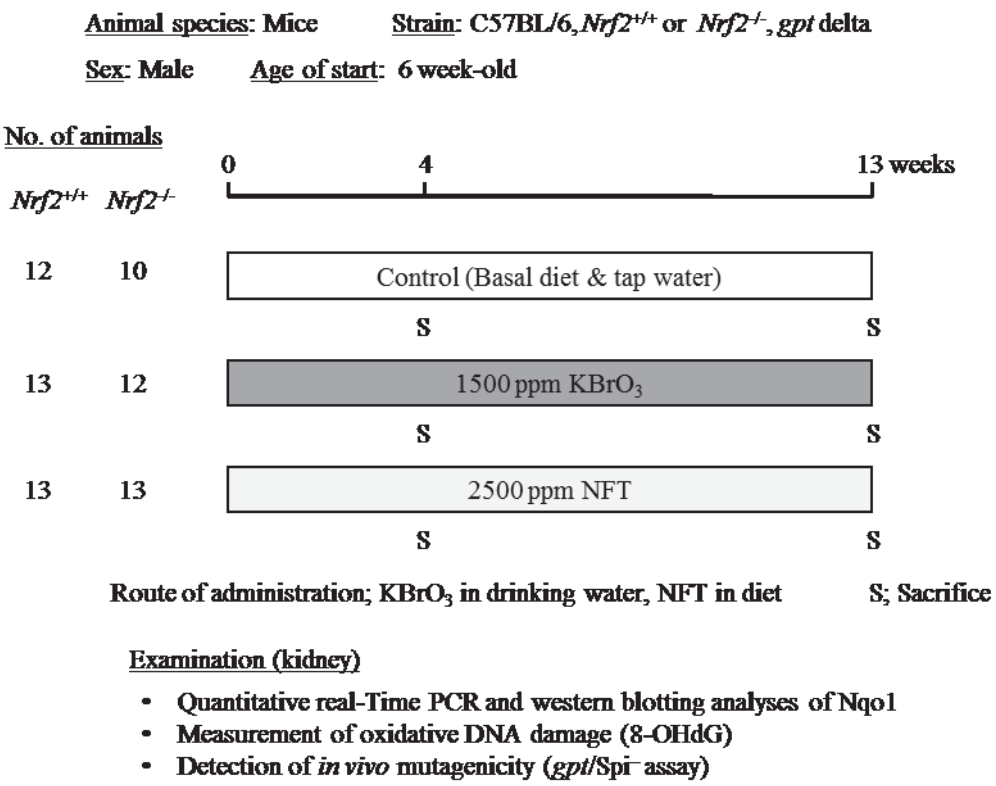

Fig. 6. Experimental design

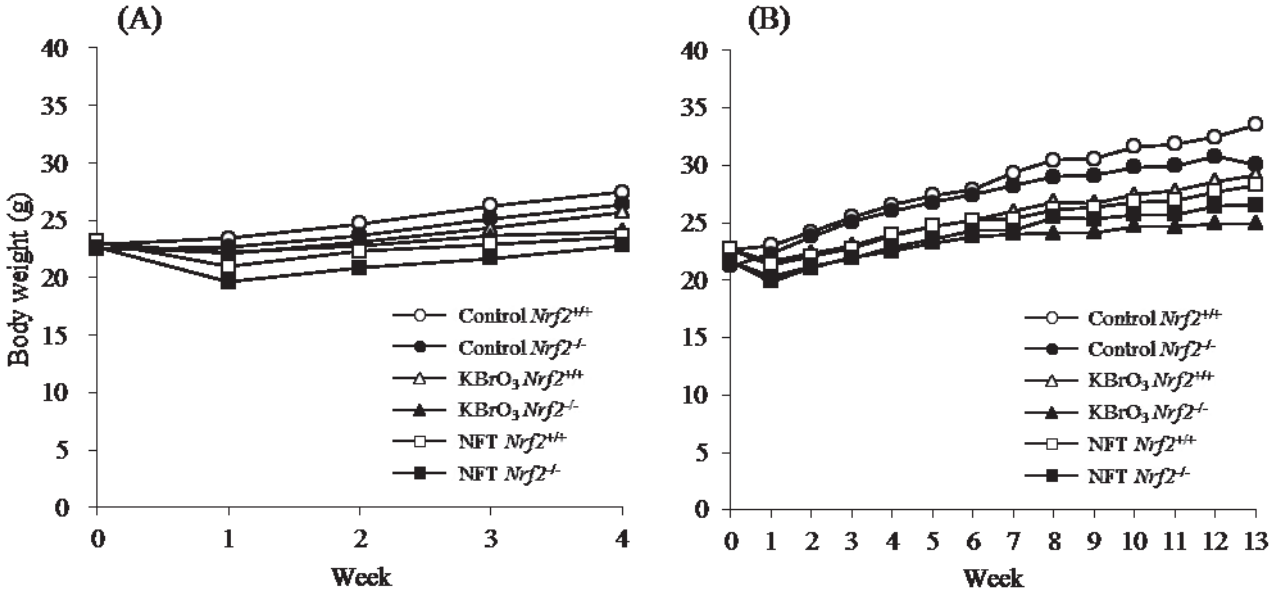

Fig. 7. Growth curves for *Nrf2*$^{+/+}$ or *Nrf2*$^{-/-}$ mice treated with $KBrO_3$ or NFT for 4 weeks (A) or 13 weeks (B). 4 to 8 mice are used in each group. For both genotypes, there were no significant differences in body weight between treated and untreated mice in either time point.

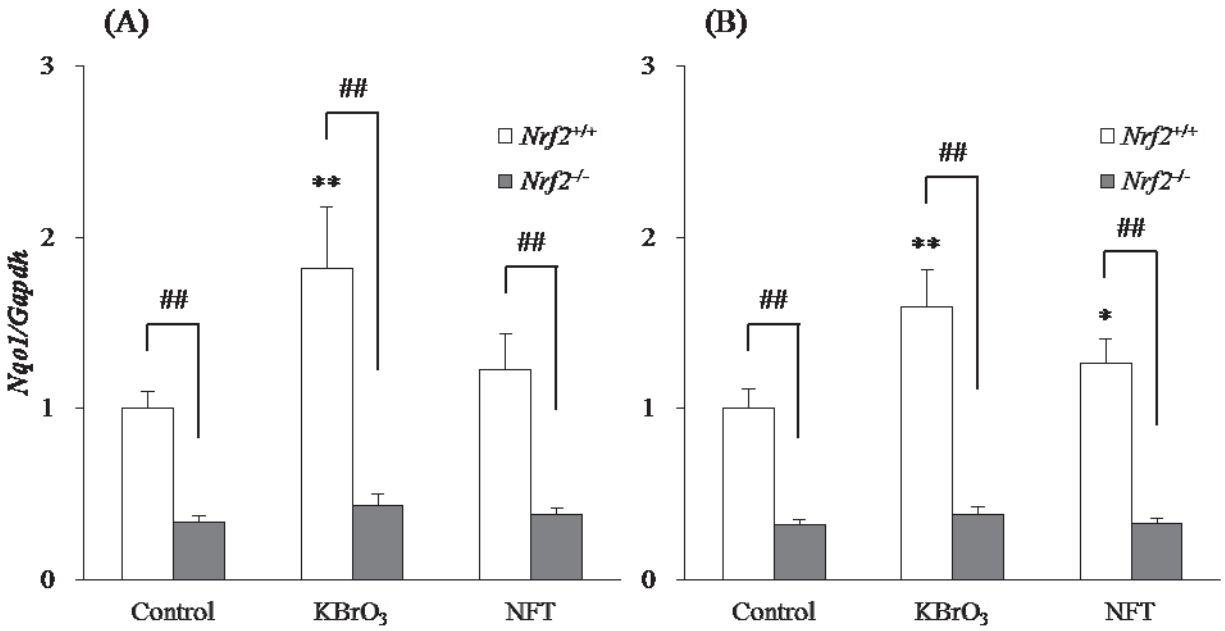

Fig. 8. Changes in mRNA levels of *Nrf2*-target gene *Nqo1* in the kidneys of $Nrf2^{+/+}$ or $Nrf2^{-/-}$ mice treated with $KBrO_3$ or NFT for 4 weeks (A) or 13 weeks (B). Data are presented as means ± SD. n=4 or 5/group. **,*: Significantly different ($P < 0.01$, 0.05) from respective control group. ##: Significantly different ($P < 0.01$) from respective $Nrf2^{+/+}$ animals.

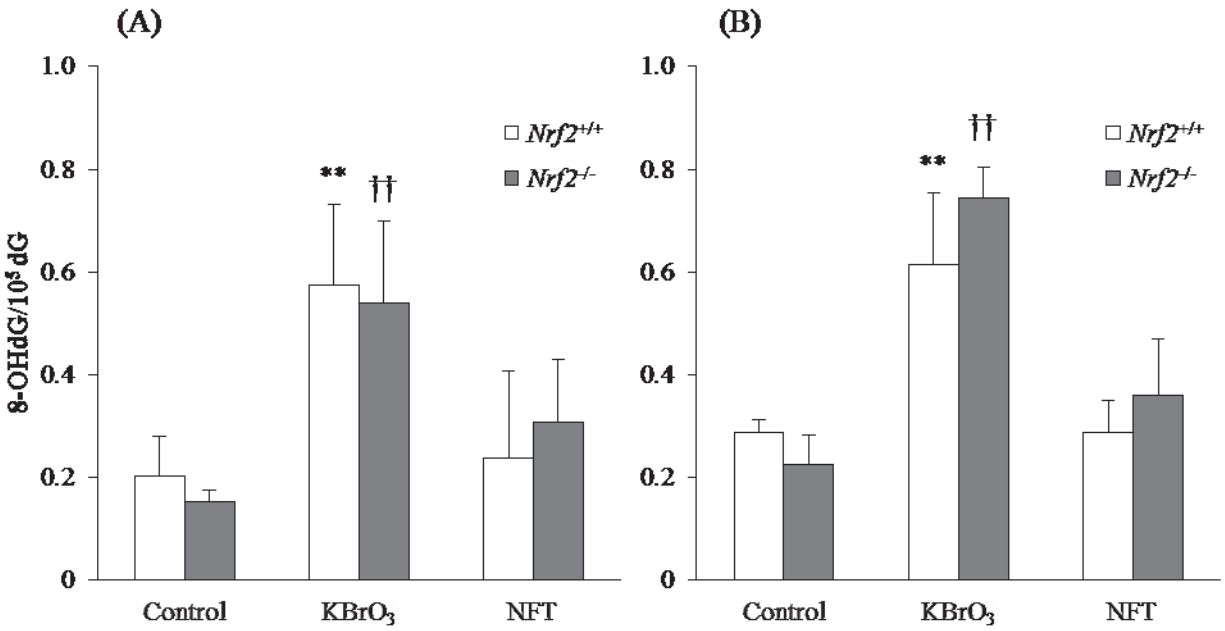

Fig. 9. 8-OHdG levels in the kidneys of *Nrf2*$^{+/+}$ or *Nrf2*$^{-/-}$ mice treated with $KBrO_3$ or NFT for 4 weeks (A) or 13 weeks (B). Data are presented as means ± SD. n=3 to 5/group. **, ††: Significantly different ($P < 0.01$) from respective control group.

Table 6. Final body and kidney weights of male *Nrf2* $^{+/+}$ or *Nrf2* $^{-/-}$ *gpt* delta mice treated with $KBrO_3$ or NFT for 4 or 13 weeks

	4 weeks					
	Nrf2 $^{+/+}$			*Nrf2* $^{-/-}$		
	Control	1,500 ppm $KBrO_3$	2,500 ppm NFT	Control	1,500 ppm $KBrO_3$	2,500 ppm NFT
No. of animals	4	5	5	4	4	5
Final body weights (g)	27.43 ± 2.59[b]	25.70 ± 2.35	23.56 ± 2.15	26.40 ± 2.18	24.05 ± 1.26	22.80 ± 1.46
Kidneys (g)	0.33 ± 0.03	0.32 ± 0.04	0.33 ± 0.04	0.32 ± 0.03	0.32 ± 0.04	0.32 ± 0.04
Kidneys (g%)[a]	1.22 ± 0.11	1.26 ± 0.09	1.38 ± 0.06	1.20 ± 0.10	1.32 ± 0.16	1.38 ± 0.13

	13 weeks					
	Nrf2 $^{+/+}$			*Nrf2* $^{-/-}$		
	Control	1,500 ppm $KBrO_3$	2,500 ppm NFT	Control	1,500 ppm $KBrO_3$	2,500 ppm NFT
No. of animals	8	8	8	6	8	8
Final body weights (g)	33.53 ± 3.45	29.18 ± 2.45	28.28 ± 1.67	30.05 ± 2.38	24.91 ± 1.80	26.55 ± 1.39
Kidneys (g)	0.35 ± 0.03	0.34 ± 0.03	0.38 ± 0.05	0.35 ± 0.05	0.34 ± 0.06	0.33 ± 0.04
Kidneys (g%)[a]	1.06 ± 0.08	1.16 ± 0.08	1.35 ± 0.12	1.18 ± 0.15	1.38 ± 0.30	1.24 ± 0.14

[a] Kidneys-to-body weight ratios (relative weights) are given as g organ weight/g body weight.

[b] Means ± SD.

Table 7. *Gpt* MFs in the kidneys of *Nrf2* $^{+/+}$ or *Nrf2* $^{-/-}$ *gpt* delta mice treated with $KBrO_3$ or NFT for 4 weeks

Genotype	Treatment	Animal No.	Cm^R colonies ($\times 10^5$)	6-TG^R and Cm^R colonies	MF ($\times 10^{-5}$)	Mean ± SD
Nrf2 $^{+/+}$	Control	101	14.4	6	0.42	
		102	41.2	10	0.24	
		103	20.0	9	0.45	
		104	41.0	13	0.32	0.36 ± 0.09
	1,500 ppm $KBrO_3$	201	32.1	30	0.93	
		202	24.2	17	0.70	
		203	23.7	18	0.76	
		204	21.5	9	0.42	
		205	17.6	12	0.68	0.70 ± 0.19 *
	2,500 ppm NFT	301	34.4	11	0.32	
		302	51.4	15	0.29	
		303	38.4	18	0.47	
		304	18.2	16	0.88	
		305	18.1	14	0.77	0.55 ± 0.27
Nrf2 $^{-/-}$	Control	401	40.7	14	0.34	
		402	34.0	13	0.38	
		403	35.4	13	0.37	
		404	18.7	4	0.21	0.33 ± 0.08
	1,500 ppm $KBrO_3$	501	24.5	17	0.69	
		502	31.1	22	0.71	
		503	15.3	9	0.59	
		504	29.1	11	0.38	0.59 ± 0.15
	2,500 ppm NFT	601	23.9	14	0.59	
		602	27.7	17	0.61	
		603	29.7	17	0.57	
		604	28.8	15	0.52	
		605	24.3	11	0.45	0.55 ± 0.06

* $P < 0.05$ vs. respective control group

Cm^R, chloramphenicol resistant; 6-TG^R, 6-thioguanine resistant; MF, mutant frequency

Table 8. *Gpt* MFs in the kidneys of *Nrf2* $^{+/+}$ or *Nrf2* $^{-/-}$ *gpt* delta mice treated with $KBrO_3$ for 13 weeks

Genotype	Treatment	Animal No.	Cm^R colonies ($\times 10^5$)	6-TG^R and Cm^R colonies	MF ($\times 10^{-5}$)	Mean ± SD
Nrf2 $^{+/+}$	Control	701	8.9	3	0.34	
		702	13.1	9	0.69	
		703	7.4	11	1.48	
		704	7.4	9	1.22	
		705	9.5	4	0.42	
		706	16.6	9	0.54	
		707	15.0	6	0.40	
		708	17.5	7	0.40	0.69 ± 0.43
	1,500 ppm $KBrO_3$	801	12.8	22	1.72	
		802	17.1	20	1.17	
		803	17.8	26	1.46	
		804	11.3	22	1.95	
		805	13.6	41	3.01	
		806	10.3	9	0.87	
		807	21.8	25	1.15	
		808	17.4	22	1.27	1.57 ± 0.67**
Nrf2 $^{-/-}$	Control	1001	15.2	9	0.59	
		1002	16.3	8	0.49	
		1003	27.3	8	0.29	
		1004	24.0	7	0.29	
		1005	18.4	13	0.71	0.48 ± 0.18
	1,500 ppm $KBrO_3$	1101	9.9	22	2.23	
		1102	23.8	41	1.72	
		1103	6.6	21	3.17	
		1104	10.2	26	2.56	
		1105	13.3	24	1.81	
		1106	18.0	23	1.28	
		1107	14.0	19	1.36	
		1108	8.4	6	0.71	1.86 ± 0.78††

** $P < 0.01$ vs. respective control group, †† $P < 0.01$ vs. respective control group

Cm^R, chloramphenicol resistant; 6-TG^R, 6-thioguanine resistant; MF, mutant frequency

Table 9. *Gpt* MFs in the kidneys of *Nrf2* $^{+/+}$ or *Nrf2* $^{-/-}$ *gpt* delta mice treated with NFT for 13 weeks

Genotype	Treatment	Animal No.	Cm^R colonies ($\times 10^5$)	6-TG^R and Cm^R colonies	MF ($\times 10^{-5}$)	Mean ± SD
Nrf2 $^{+/+}$	Control	701	8.4	6	0.72	
		702	9.2	5	0.54	
		703	11.0	3	0.27	
		704	13.6	4	0.29	
		705	10.6	4	0.38	
		706	21.3	6	0.28	
		707	19.6	4	0.20	
		708	24.5	9	0.37	0.38 ± 0.17
	2,500 ppm NFT	901	15.3	21	1.37	
		902	13.5	10	0.74	
		903	16.2	12	0.74	
		904	12.0	13	1.09	
		905	11.0	14	1.27	
		906	24.3	24	0.99	
		907	14.3	16	1.12	1.04 ± 0.24**
Nrf2 $^{-/-}$	Control	1001	15.2	5	0.33	
		1002	13.3	8	0.60	
		1003	28.3	11	0.39	
		1004	24.2	9	0.37	
		1005	22.9	6	0.26	0.39 ± 0.13
	2,500 ppm NFT	1201	13.1	21	1.60	
		1202	18.8	22	1.17	
		1203	21.6	22	1.02	
		1204	13.2	15	1.13	
		1205	12.3	15	1.22	
		1206	7.6	12	1.58	
		1207	12.3	22	1.79	
		1208	13.6	23	1.69	1.40 ± 0.30††

** $P < 0.01$ vs. respective control group, †† $P < 0.01$ vs. respective control group

Cm^R, chloramphenicol resistant; 6-TG^R, 6-thioguanine resistant; MF, mutant frequency

Table 10. Mutation spectra of *gpt* mutant colonies in the kidneys of *Nrf2* $^{+/+}$ or *Nrf2* $^{-/-}$ *gpt* delta mice treated with $KBrO_3$ or NFT for 4 weeks

	Nrf2 $^{+/+}$					
	Control		1,500 ppm $KBrO_3$		2,500 ppm NFT	
	Number (%)	Mutation frequencies (10^{-5})	Number (%)	Mutation frequencies (10^{-5})	Number (%)	Mutation frequencies (10^{-5})
Base substitution						
Transversions						
G:C-T:A	7 (18.4)	0.06 ± 0.03	16 (18.6)	0.13 ± 0.04	16 (21.6)	0.12 ± 0.07
G:C-C:G	2 (5.3)	0.02 ± 0.03	2 (2.3)	0.01 ± 0.02	7 (9.5)	0.05 ± 0.03
A:T-T:A	2 (5.3)	0.02 ± 0.02	10 (11.6)	0.08 ± 0.05	2 (2.7)	0.01 ± 0.02
A:T-C:G	0	0	2 (2.3)	0.02 ± 0.03	4 (5.4)	0.03 ± 0.05
Transitions						
G:C-A:T	15 (39.5)	0.13 ± 0.02	17 (19.8)	0.14 ± 0.07	26 (35.1)	0.18 ± 0.07
A:T-G:C	2 (5.3)	0.02 ± 0.03	6 (7.0)	0.05 ± 0.03	4 (5.4)	0.03 ± 0.02
Deletion						
Single bp	5 (13.2)	0.05 ± 0.04	16 (18.6)	0.13 ± 0.05	10 (13.5)	0.08 ± 0.06
Over 2bp	2 (5.3)	0.02 ± 0.02	7 (8.1)	0.05 ± 0.04	3 (4.1)	0.02 ± 0.02
Insertion	1 (2.6)	0.01 ± 0.01	7 (8.1)	0.05 ± 0.04 *	0	0
Complex	2 (5.3)	0.02 ± 0.02	3 (3.5)	0.03 ± 0.05	2 (2.7)	0.02 ± 0.05
Total	38	0.36	86	0.70	74	0.55

	Nrf2 $^{-/-}$					
	Control		1,500 ppm $KBrO_3$		2,500 ppm NFT	
	Number (%)	Mutation frequencies (10^{-5})	Number (%)	Mutation frequencies (10^{-5})	Number (%)	Mutation frequencies (10^{-5})
Base substitution						
Transversions						
G:C-T:A	7 (15.9)	0.06 ± 0.03	6 (10.2)	0.05 ± 0.04	19 (25.7)	0.14 ± 0.07
G:C-C:G	2 (4.5)	0.01 ± 0.02	3 (5.1)	0.03 ± 0.03	5 (6.8)	0.04 ± 0.03
A:T-T:A	0	0	7 (11.9)	0.06 ± 0.08	6 (8.1)	0.04 ± 0.05
A:T-C:G	2 (4.5)	0.02 ± 0.03	1 (1.7)	0.01 ± 0.02	2 (2.7)	0.02 ± 0.02
Transitions						
G:C-A:T	20 (45.5)	0.14 ± 0.06	10 (16.9)	0.10 ± 0.03	22 (29.7)	0.16 ± 0.02
A:T-G:C	2 (4.5)	0.01 ± 0.02	5 (8.5)	0.05 ± 0.02	5 (6.8)	0.04 ± 0.04
Deletion						
Single bp	6 (13.6)	0.04 ± 0.04	19 (32.2)	0.21 ± 0.09 ††	11 (14.9)	0.08 ± 0.05
Over 2bp	1 (2.3)	0.01 ± 0.01	5 (8.5)	0.06 ± 0.06	1 (1.4)	0.01 ± 0.02
Insertion	1 (2.3)	0.01 ± 0.01	2 (3.4)	0.02 ± 0.02	2 (2.7)	0.01 ± 0.02
Complex	3 (6.8)	0.02 ± 0.01	1 (1.7)	0.01 ± 0.02	1 (1.4)	0.01 ± 0.02
Total	44	0.33	59	0.59	74	0.55

* $P < 0.05$ vs. respective control group, †† $P < 0.01$ vs. respective control group

Table 11. Mutation spectra of *gpt* mutant colonies in the kidneys of *Nrf2* $^{+/+}$ or *Nrf2* $^{-/-}$ *gpt* delta mice treated with $KBrO_3$ for 13 weeks

	Nrf2 $^{+/+}$				*Nrf2* $^{-/-}$			
	Control		1,500 ppm $KBrO_3$		Control		1,500 ppm $KBrO_3$	
	Number (%)	Mutation frequencies (10^{-5})	Number (%)	Mutation frequencies (10^{-5})	Number (%)	Mutation frequencies (10^{-5})	Number (%)	Mutation frequencies (10^{-5})
Base substitution								
Transversions								
G:C-T:A	15 (25.9)	0.18 ± 0.16	20 (10.7)	0.16 ± 0.11	13 (28.9)	0.13 ± 0.06	15 (8.2)	0.15 ± 0.11
G:C-C:G	2 (3.4)	0.03 ± 0.06	5 (2.7)	0.04 ± 0.05	1 (2.2)	0.01 ± 0.02	2 (1.1)	0.02 ± 0.03
A:T-T:A	0	0	11 (5.9)	0.10 ± 0.11*	3 (6.7)	0.03 ± 0.03	28 (15.4)	0.27 ± 0.16†
A:T-C:G	0	0	10 (5.3)	0.07 ± 0.06**	0	0	1 (0.5)	0.01 ± 0.03
Transitions								
G:C-A:T	19 (32.8)	0.22 ± 0.21	33 (17.6)	0.27 ± 0.13	19 (42.2)	0.20 ± 0.08	27 (14.8)	0.29 ± 0.16
A:T-G:C	4 (6.9)	0.05 ± 0.08	7 (3.7)	0.06 ± 0.09	3 (6.7)	0.04 ± 0.03	4 (2.2)	0.05 ± 0.06
Deletion								
Single bp	11 (19.0)	0.12 ± 0.11	69 (36.9)	0.60 ± 0.34**	3 (6.7)	0.03 ± 0.03	62 (34.1)	0.65 ± 0.41††
Over 2bp	2 (3.4)	0.03 ± 0.05	20 (10.7)	0.17 ± 0.07**	1 (2.2)	0.01 ± 0.03	29 (15.9)	0.30 ± 0.13††
Insertion	4 (6.9)	0.04 ± 0.07	8 (4.3)	0.07 ± 0.07	1 (2.2)	0.01 ± 0.02	6 (3.3)	0.06 ± 0.10
Complex	1 (1.7)	0.01 ± 0.02	4 (2.1)	0.03 ± 0.04	1 (2.2)	0.01 ± 0.03	8 (4.4)	0.07 ± 0.05†
Total	58	0.69	187	1.57	45	0.48	182	1.86

**, * $P < 0.01, 0.05$ vs. respective control group, ††, † $P < 0.01, 0.05$ vs. respective control group

Table 12. Mutation spectra of *gpt* mutant colonies in the kidneys of *Nrf2* $^{+/+}$ or *Nrf2* $^{-/-}$ *gpt* delta mice treated with NFT for 13 weeks

	Nrf2 $^{+/+}$				*Nrf2* $^{-/-}$			
	Control		2,500 ppm NFT		Control		2,500 ppm NFT	
	Number (%)	Mutation frequencies (10^{-5})	Number (%)	Mutation frequencies (10^{-5})	Number (%)	Mutation frequencies (10^{-5})	Number (%)	Mutation frequencies (10^{-5})
Base substitution								
Transversions								
G:C-T:A	9 (22.0)	0.08 ± 0.07	31 (28.2)	0.29 ± 0.05**	8 (20.5)	0.07 ± 0.05	47 (30.9)	0.43 ± 0.15††
G:C-C:G	4 (9.8)	0.04 ± 0.05	28 (25.5)	0.26 ± 0.06**	3 (7.7)	0.02 ± 0.03	38 (25.0)	0.37 ± 0.17††
A:T-T:A	0	0	5 (4.5)	0.05 ± 0.07	1 (2.6)	0.01 ± 0.02	7 (4.6)	0.07 ± 0.06†
A:T-C:G	1 (2.4)	0.01 ± 0.02	2 (1.8)	0.02 ± 0.04	0	0	3 (2.0)	0.02 ± 0.03
Transitions								
G:C-A:T	19 (46.3)	0.18 ± 0.10	26 (23.6)	0.24 ± 0.12	16 (41.0)	0.17 ± 0.07	27 (17.8)	0.25 ± 0.09
A:T-G:C	1 (2.4)	0.01 ± 0.02	4 (3.6)	0.04 ± 0.04	0	0	3 (2.0)	0.03 ± 0.04
Deletion								
Single bp	4 (9.8)	0.04 ± 0.04	7 (6.4)	0.06 ± 0.05	9 (23.1)	0.09 ± 0.09	10 (6.6)	0.09 ± 0.05
Over 2bp	2 (4.9)	0.03 ± 0.05	2 (1.8)	0.02 ± 0.03	1 (2.6)	0.02 ± 0.03	3 (2.0)	0.03 ± 0.04
Insertion	0	0	1 (0.9)	0.01 ± 0.02	1 (2.6)	0.01 ± 0.02	5 (3.3)	0.04 ± 0.06
Complex	1 (2.4)	0.01 ± 0.03	4 (3.6)	0.04 ± 0.07	0	0	9 (5.9)	0.08 ± 0.10
Total	41	0.38	110	1.04	39	0.39	152	1.40

** $P < 0.01$ vs. respective control group, ††, † $P < 0.01, 0.05$ vs. respective control group

Table 13. Spi⁻ MFs in the kidneys of *Nrf2* $^{+/+}$ or *Nrf2* $^{-/-}$ *gpt* delta mice treated with $KBrO_3$ or NFT for 4 weeks

Genotype	Treatment	Animal No.	Plaques within XL-1 Blue MRA ($\times 10^5$)	Plaques within XL-1 Blue MRA (P2)	MF ($\times 10^{-5}$)	Mean ± SD
Nrf2 $^{+/+}$	Control	101	24.6	8	0.33	
		102	43.7	4	0.09	
		103	16.9	3	0.18	
		104	24.2	9	0.37	0.24 ± 0.13
	1,500 ppm $KBrO_3$	201	33.5	22	0.66	
		202	30.2	12	0.40	
		203	31.7	13	0.41	
		204	38.9	8	0.21	
		205	21.4	10	0.47	0.43 ± 0.16
	2,500 ppm NFT	301	38.4	7	0.18	
		302	44.1	15	0.34	
		303	33.8	12	0.36	
		304	27.2	13	0.48	
		305	19.9	3	0.15	0.30 ± 0.13
Nrf2 $^{-/-}$	Control	401	64.5	11	0.17	
		402	24.7	3	0.12	
		403	29.0	7	0.24	
		404	19.8	4	0.20	0.18 ± 0.05
	1,500 ppm $KBrO_3$	501	19.5	9	0.46	
		502	36.5	9	0.25	
		503	19.2	6	0.31	
		504	23.3	10	0.43	0.36 ± 0.10
	2,500 ppm NFT	601	25.6	6	0.23	
		602	34.4	7	0.20	
		603	30.1	6	0.20	
		604	27.8	10	0.36	
		605	29.4	9	0.31	0.26 ± 0.07

MF: mutant frequency

Table 14. Spi⁻ MFs in the kidneys fof *Nrf2* $^{+/+}$ or *Nrf2* $^{-/-}$ *gpt* delta mice treated with $KBrO_3$ or NFT for 13 weeks

Genotype	Treatment	Animal No.	Plaques within XL-1 Blue MRA ($\times 10^5$)	Plaques within XL-1 Blue MRA (P2)	MF ($\times 10^{-5}$)	Mean ± SD
Nrf2 $^{+/+}$	Control	701	31.0	13	0.42	
		702	37.5	11	0.29	
		703	23.7	5	0.21	
		704	26.5	9	0.34	
		705	20.8	6	0.29	
		706	27.9	9	0.32	
		707	22.9	7	0.31	
		708	46.9	13	0.28	0.31 ± 0.06
	1,500 ppm $KBrO_3$	801	49.8	45	0.90	
		802	16.1	16	0.99	
		803	42.0	32	0.76	
		804	25.0	26	1.04	
		805	29.6	30	1.01	
		806	16.6	12	0.72	
		807	12.9	10	0.78	
		808	26.0	16	0.62	0.85 ± 0.16 **
	2,500 ppm NFT	901	40.5	14	0.35	
		902	6.5	2	0.31	
		903	24.3	8	0.33	
		904	16.5	4	0.24	
		905	18.3	7	0.31	
		906	22.7	4	0.32	
		907	12.3	8	0.46	0.33 ± 0.07
Nrf2 $^{-/-}$	Control	1001	32.2	8	0.25	
		1002	33.2	7	0.21	
		1003	43.6	14	0.32	
		1004	22.2	8	0.36	
		1005	31.7	9	0.28	0.28 ± 0.06
	1,500 ppm $KBrO_3$	1101	26.9	18	0.67	
		1102	35.6	45	1.26	
		1103	15.9	18	1.13	
		1104	30.0	18	0.60	
		1105	20.6	21	1.02	
		1106	14.3	14	0.98	
		1107	29.3	16	0.55	
		1108	6.0	7	1.16	0.92 ± 0.28 ††
	2,500 ppm NFT	1201	31.2	12	0.38	
		1202	22.0	6	0.27	
		1203	35.5	14	0.39	
		1204	23.5	4	0.17	
		1205	19.7	11	0.56	
		1206	17.3	7	0.41	
		1207	21.3	11	0.52	
		1208	28.4	6	0.21	0.36 ± 0.14

** $P < 0.01$ vs. respective control group, †† $P < 0.01$ vs. respective control group
MF, mutant frequency

Table 15. Mutation spectra of Spi^- plaques in the kidneys of *Nrf2* $^{+/+}$ or *Nrf2* $^{-/-}$ *gpt* delta mice treated with $KBrO_3$ or NFT for 4 weeks

		Nrf2 $^{+/+}$					
		Control		1,500 ppm $KBrO_3$		2,500 ppm NFT	
		Number (%)	Mutation frequencies (10^{-5})	Number (%)	Mutation frequencies (10^{-5})	Number (%)	Mutation frequencies (10^{-5})
Single bp deletion							
Simple	G or C	6 (25.0)	0.06 ± 0.04	6 (9.2)	0.04 ± 0.05	6 (12.0)	0.03 ± 0.03
	A or T	0	0	5 (7.7)	0.03 ± 0.04	1 (2.0)	0.01 ± 0.01
In run	G or C	4 (16.7)	0.04 ± 0.03	17 (26.2)	0.12 ± 0.08	15 (30.0)	0.09 ± 0.09
	A or T	5 (20.8)	0.05 ± 0.03	18 (27.7)	0.11 ± 0.09	13 (26.0)	0.08 ± 0.04
2 to 1 kb deletion		0	0	5 (7.7)	0.03 ± 0.04	0	0
Over 1 kb deletion		8 (33.3)	0.08 ± 0.10	12 (18.5)	0.08 ± 0.11	12 (24.0)	0.07 ± 0.07
Complex		1 (4.2)	0.01 ± 0.02	2 (3.1)	0.01 ± 0.03	1 (2.0)	0.01 ± 0.01
Insertion		0	0	0	0	1 (2.0)	0.01 ± 0.02
Base substitution		0	0	0	0	1 (2.0)	0.00 ± 0.01
Total		24	0.24	65	0.43	50	0.30

		Nrf2 $^{-/-}$					
		Control		1,500 ppm $KBrO_3$		2,500 ppm NFT	
		Number (%)	Mutation frequencies (10^{-5})	Number (%)	Mutation frequencies (10^{-5})	Number (%)	Mutation frequencies (10^{-5})
Single bp deletion							
Simple	G or C	0	0	7 (20.6)	0.08 ± 0.05	3 (7.9)	0.02 ± 0.02
	A or T	2 (8.0)	0.01 ± 0.02	2 (5.9)	0.02 ± 0.02	0	0
In run	G or C	7 (28.0)	0.04 ± 0.03	9 (26.5)	0.10 ± 0.09	12 (31.6)	0.08 ± 0.05
	A or T	8 (32.0)	0.06 ± 0.08	8 (23.5)	0.09 ± 0.06	11 (28.9)	0.08 ± 0.05
2 to 1 kb deletion		0	0	3 (8.8)	0.03 ± 0.04	0	0
Over 1 kb deletion		8 (32.0)	0.07 ± 0.06	4 (11.8)	0.04 ± 0.04	12 (31.6)	0.08 ± 0.05
Complex		0	0	1 (2.9)	0.01 ± 0.01	0	0
Insertion		0	0	0	0	0	0
Base substitution		0	0	0	0	0	0
Total		25	0.18	34	0.36	38	0.26

Table 16. Mutation spectra of Spi$^-$ plaques in the kidneys of *Nrf2* $^{+/+}$ or *Nrf2* $^{-/-}$ *gpt* delta mice treated with $KBrO_3$ or NFT for 13 weeks

		Nrf2 $^{+/+}$					
		Control		1,500 ppm $KBrO_3$		2,500 ppm NFT	
		Number (%)	Mutation frequencies (10^{-5})	Number (%)	Mutation frequencies (10^{-5})	Number (%)	Mutation frequencies (10^{-5})
Single bp deletion							
Simple	G or C	10 (13.7)	0.04 ± 0.03	24 (12.8)	0.11 ± 0.07*	6 (12.8)	0.05 ± 0.05
	A or T	2 (2.7)	0.01 ± 0.02	13 (7.0)	0.05 ± 0.04*	2 (4.3)	0.01 ± 0.02
In run	G or C	20 (27.4)	0.09 ± 0.05	60 (32.1)	0.27 ± 0.09**	22 (46.8)	0.16 ± 0.10
	A or T	28 (38.4)	0.12 ± 0.06	63 (33.7)	0.29 ± 0.10**	10 (21.3)	0.06 ± 0.06
2 to 1 kb deletion		1 (1.4)	0.00 ± 0.01	12 (6.4)	0.05 ± 0.05*	0	0
Over 1 kb deletion		12 (16.4)	0.05 ± 0.03	15 (8.0)	0.08 ± 0.06	4 (8.5)	0.02 ± 0.03
Complex		0	0	0	0	1 (2.1)	0.00 ± 0.01
Insertion		0	0	0	0	0	0
Base substitution		0	0	0	0	2 (4.3)	0.01 ± 0.03
Total		73	0.31	187	0.85	47	0.33

		Nrf2 $^{-/-}$					
		Control		1,500 ppm $KBrO_3$		2,500 ppm NFT	
		Number (%)	Mutation frequencies (10^{-5})	Number (%)	Mutation frequencies (10^{-5})	Number (%)	Mutation frequencies (10^{-5})
Single bp deletion							
Simple	G or C	13 (28.3)	0.09 ± 0.07	17 (10.8)	0.10 ± 0.09	5 (7.0)	0.03 ± 0.05
	A or T	1 (2.2)	0.00 ± 0.01	15 (9.6)	0.10 ± 0.11†	3 (4.2)	0.02 ± 0.02
In run	G or C	6 (13.0)	0.04 ± 0.03	44 (28.0)	0.23 ± 0.09††	24 (33.8)	0.12 ± 0.07†
	A or T	22 (47.8)	0.13 ± 0.07	50 (31.8)	0.31 ± 0.13†	20 (28.2)	0.10 ± 0.06
2 to 1 kb deletion		0	0	19 (12.1)	0.13 ± 0.09††	3 (4.2)	0.02 ± 0.03
Over 1 kb deletion		4 (8.7)	0.02 ± 0.04	11 (7.0)	0.05 ± 0.07	14 (19.7)	0.08 ± 0.07
Complex		0	0	0	0	0	0
Insertion		0	0	0	0	1 (1.4)	0.01 ± 0.02
Base substitution		0	0	1 (0.6)	0.00 ± 0.01	1 (1.4)	0.00 ± 0.01
Total		46	0.28	157	0.92	71	0.36

**, * $P < 0.01, 0.05$ vs. respective control group, ††, † $P < 0.01, 0.05$ vs. respective control group

General Discussion

Nrf2-deficient animal model

Nqo1 encodes NAD(P)H:quinone oxidoreductase 1 (NQO1), whose enzymatic activity avoids the one electron reduction of quinones that results in the production of radical species (6). In this way, NQO1 has broad effects and protects cells from kinds of stresses including radicals (6). The fact that the expression level of *Nqo1* did not increase by the enough exposure of NFT or $KBrO_3$ in the kidney of *Nrf2*$^{-/-}$ mice in the present study clearly suggested that *Nrf2*$^{-/-}$ mice were affected more severely by oxidative stress than *Nrf2*$^{+/+}$ mice. The degree of 8-OHdG level increase by $KBrO_3$ in *Nrf2*$^{-/-}$ mice was higher than that in *Nrf2*$^{+/+}$ mice also implied the lack of defense mechanism against oxidative stress. Thus, *Nrf2*$^{-/-}$ mice in the present study showed hypersensitivity to oxidative stress, and it was confirmed that this hypersensitive animal model was useful for the investigation of oxidative stress on the diseases *in vivo*. Furthermore, considering that oxidative stress is also related to the progression of inflammation and other pathological conditions (12, 31), this hypersensitive animal model might be useful for not only the investigation of oxidative stress-induced carcinogenesis but that of inflammation-related disease and so on.

Role of oxidative stress in NFT-induced carcinogenesis

The results in the present study demonstrated that the side chains may influence the generation of oxidative stress by the nitro-reduction of the nitro group in NFT-induced carcinogenesis. In general, the existence of nitro group is simply

considered as a key factor of the potential to induce oxidative stress. However, the results about NFT and its constituent moieties in the present and the previous studies clearly suggested the difficulty of prediction of oxidative stress inducing potential and the risk of oxidative stress-related carcinogenesis (27). Even though oxidative stress plays an important role in carcinogenesis in nitrofurans including NFT, the direct effect to DNA such as the formation of DNA adduct should be considered as another notable factor in carcinogenesis by nitrofurans (48, 51). Actually, the increase of 8-OHdG and MFs did not correlate in the NFA-treated animals. For these reasons, I would like to propose that the oxidative stress induced by side chain binding and the direct damage to DNA should be considered also in the risk assessment and during the development of new nitrofuran compounds. In addition, no change in 8-OHdG in NFT-treated *Nrf2*$^{+/+}$ mice, unlike in rats (27), indicates that the sensitivity to oxidative stress is greater in rats than in mice; this may explain the difference in NFT carcinogenicity between rats and mice. These facts might imply the impact of oxidative stress in the chemical-induced renal carcinogenesis at the same time.

Role of oxidative stress in $KBrO_3$-induced carcinogenesis

$KBrO_3$ has a strong potential as an oxidant agent, and exerts the oxidizing power by the release of bromine radicals (36). They oxidize many kinds of proteins, lipids, and nucleic acids, then increase the level of thiobarbituric acid-reactive substances (TBARS), 8-OHdG, and so on. The mechanisms of action in $KBrO_3$-induced carcinogenesis had been investigated in the previous studies, which demonstrated that

the oxidative DNA damage, subsequent gene mutations, and the stimulation of cell proliferation are prominent factors *in vivo* (53, 55, 56, 59). Because of these function, $KBrO_3$ has the potential of an initiator and a promoter (53). *In vitro* studies also showed the induction of 8-OHdG by $KBrO_3$, and suggested that 8-OHdG plays a key role in $KBrO_3$-induced mutagenesis and carcinogenesis (1). Furthermore, the present study showed the importance of the oxidative DNA damage especially 8-OHdG in $KBrO_3$-induced mutagenesis, and the deletion mutations were the characteristic type of mutations induced by $KBrO_3$ as previously described (55). The new findings in the present study were the increases of the deletion size accompanied with the elevations of MFs and 8-OHdG level in *Nrf2*$^{-/-}$ mice. An *in vitro* report demonstrated that error in the repair process of 8-OHdG caused double-strand breaks (DSBs) in human cells, and DSBs resulted in the large deletion (33). Considering these mechanisms, the present results strongly support the consideration that 8-OHdG induced by the oxidizing potential of $KBrO_3$ directly involved in the increase of deletion mutations.

Impact of the formation of 8-OHdG in chemical induced carcinogenesis

8-OHdG, a major oxidized DNA lesion, has been frequently utilized as a marker of oxidative stress in not only academic research but in clinical practice; prediction of the risk of cardiovascular disease, cancer, life style diseases, and so on (5, 19). Measurement of 8-OHdG in the tissue samples of experimental animals gave the direct information of oxidative stress in the target organs in the studies for the mechanisms of action of oxidative stress in some diseases. However, considering the

risk assessment of oxidative stress, the impact of the formation of 8-OHdG seems to be different in each chemical substance. Actually, high dose administration of NFT by gavage showed the elevation of 8-OHdG levels in the kidneys accompanied with the increase of MFs, but lower exposure in diet did not change 8-OHdG levels despite of increase of MFs. On the other hand, the results of $KBrO_3$ in the present study indicated the direct relationship between the formation of 8-OHdG and deletion mutations in $KBrO_3$ exposure as stated previously (55). In $KBrO_3$-induced mutagenesis, the formation of high amount of 8-OHdG leads to the errors of repair systems such as base excision repair, and the errors might result in subsequent gene mutations.

Risk assessment of oxidative stress

In our surroundings, there are many chemical substances, and some of them have the potential to produce oxidative stress. In the risk assessment of environmental chemical substances, investigations about the detailed mechanisms including oxidative stress seem to be necessary. Previous studies have suggested that oxidative stress might function in some diseases including cancer (12, 31, 46, 47, 53). In the present study, I demonstrated the different modes of involvement of oxidative stress by two chemical substances which are ingested by humans through the diet: NFT and $KBrO_3$. The present study leads to accurate risk assessment of oxidative stress in carcinogenicity by environmental chemical substances, and I will further progress research about oxidative stress.

Conclusion

The present study focused on the involvement of oxidative stress in the mutagenesis using hypersensitive animals. Different modes of involvement of oxidative stress in two chemical substances which were ingested by humans through the diet were demonstrated. The results about NFT demonstrated that the side chain interaction was important in the generation of oxidative stress by the nitro-reduction of the nitro group, and the formation of 8-OHdG was not necessary in NFT-induced mutagenesis. The results about $KBrO_3$ demonstrated the importance of the oxidative DNA damage especially 8-OHdG and subsequent deletion mutations in $KBrO_3$-induced mutagenesis. The present study leads to accurate risk assessment of oxidative stress in carcinogenicity by environmental chemical substances.

Acknowledgements

The author extends his deepest gratitude to following persons for their help in the completion of this thesis: Dr. Takashi Umemura, and Dr. Akiyoshi Nishikawa at National Institute of Health Sciences, and Professor Dr. Tokuma Yanai at United Graduate School of Veterinary Sciences, Gifu University, for their excellent guidance and supervision; Professor Dr. Makoto Shibutani, and Associate Professor Dr. Toshinori Yoshida at Tokyo University of Agriculture and Technology, Professor Dr. Yoshiyasu Kobayashi at Obihiro University of Agriculture and Veterinary Medicine, and Professor Dr. Hiroshi Satoh at Iwate University for their important advice and assistance. I also appreciate Dr. Yuji Ishii, Dr. Shinji Takasu, Dr. Yuh Yokoo, and Ms. Aki Kijima at National Institute of Health Sciences for their important advice and assistance through the experiments and paper works.

References

1. Ballmaier D, and Epe B. Oxidative DNA damage induced by potassium bromate under cell-free conditions and in mammalian cells. Carcinogenesis. **16**: 335–342. 1995.
2. Bartel LC, Montalto de Mecca M, and Castro JA. Nitroreductive metabolic activation of some carcinogenic nitro heterocyclic food contaminants in rat mammary tissue cellular fractions. Food Chem Toxicol. **47**: 140–144. 2009.
3. Boelsterli UA, Ho HK, Zhou S, and Leow KY. Bioactivation and hepatotoxicity of nitroaromatic drugs. Curr Drug Metab. **7**: 715–727. 2006.
4. Chung MC, Bosquesi PL, and dos Santos JL. A prodrug approach to improve the physico-chemical properties and decrease the genotoxicity of nitro compounds. Curr Pharm Des. **17**: 3515–3526. 2011.
5. Di Minno A, Turnu L, Porro B, Squellerio I, Cavalca V, Tremoli E, and Di Minno MND. 8-hydroxy-2-deoxyguanosine levels and cardiovascular disease: a systematic review and meta-analysis of the literature. Antioxid Redox Signal. **24**: 548–555. 2016.
6. Dinkova-Kostova AT, and Talalay P. NAD(P)H:quinone acceptor oxidoreductase 1 (NQO1), a multifunctional antioxidant enzyme and exceptionally versatile cytoprotector. Arch Biochem Biophys. **501**: 116–123. 2010.
7. Enomoto A, Itoh K, Nagayoshi E, Haruta J, Kimura T, O'Connor T, Harada T, and Yamamoto M. High sensitivity of Nrf2 knockout mice to acetaminophen hepatotoxicity associated with decreased expression of ARE-regulated drug

metabolizing enzymes and antioxidant genes. Toxicol Sci. **59**: 169–177. 2001.

8. Fleck LE, North EJ, Lee RE, Mulcahy LR, Casadei G, and Lewis K. A screen for and validation of prodrug antimicrobials. Antimicrob Agents Chemother. **58**: 1410–1419. 2014.

9. French JE. Toxicology and carcinogenesis studies of nitrofurantoin (CAS NO. 67-20-9) in F344/N rats and B6C3F_1 mice (feed studies). 1989, from National Toxicology Program website: https://ntp.niehs.nih.gov/ntp/htdocs/lt_rpts/tr341.pdf

10. Fukushima S, Gi M, Kakehashi A, Wanibuchi H, and Matsumoto M. Qualitative and quantitative approaches in the dose-response assessment of genotoxic carcinogens. Mutagenesis. **31**: 341–346. 2016.

11. Fukushima S, Kinoshita A, Puatanachokchai R, Kushida M, Wanibuchi H, and Morimura K. Hormesis and dose-response-mediated mechanisms in carcinogenesis: evidence for a threshold in carcinogenicity of non-genotoxic carcinogens. Carcinogenesis. **26**: 1835–1845. 2005.

12. Gupte AA, Lyon CJ, and Hsueh WA. Nuclear factor (erythroid-derived 2)-like-2 factor (Nrf2), a key regulator of the antioxidant response to protect against atherosclerosis and nonalcoholic steatohepatitis. Curr Diab Rep. 13: 362–371. 2013.

13. Hayashi M, Kishi M, Sofuni T, and Ishidate M Jr. Micronucleus tests with mice on 39 food additives and 8 miscellaneous chemical substances. Chem Toxicol. **26**: 487–500. 1988.

14. Hu X, Roberts JR, Apopa PL, Kan YW, and Ma Q. Accelerated ovarian failure induced by 4-vinyl cyclohexene diepoxide in Nrf2 null mice. Mol Cell Biol. **26**: 940–954. 2006.

15. IARC Working Group on the Evaluation of the Carcinogenic Risk to Humans. Furaltadone. IARC Monographs on the Evaluation of Carcinogenic Risks to Humans, Vol. 7. Lyon. 161–169. 1974.

16. IARC Working Group on the Evaluation of the Carcinogenic Risk to Humans. Furazolidone. IARC Monographs on the Evaluation of the Carcinogenic Risk to Humans, Vol. 31. Lyon. 1983.

17. IARC Working Group on the Evaluation of the Carcinogenic Risk to Humans. Nitrofural (nitrofurazone). IARC Monographs on the Evaluation of the Carcinogenic Risks of Chemicals to Humans, Vol. 50. Lyon. 195–209. 1990.

18. IARC Working Group on the Evaluation of the Carcinogenic Risk to Humans. Nitrofurantoin. IARC Monographs on the Evaluation of the Carcinogenic Risks to Humans, Vol. 50. Lyon. 211–231. 1990.

19. Il'yasova D, Scarbrough P, and Spasojevic I.Urinary biomarker of oxidative status. Clin Chim Acta. **413**: 1446–1453. 2012.

20. Ishidate M Jr, and Yoshikawa K. Chromosome aberration tests with Chinese hamster cells in vitro with and without metabolic activation: a comparative study on mutagens and carcinogens. Arch Toxicol Supplement. **4**: 41–44. 1980.

21. Ishidate M Jr, Sofuni T, Yoshikawa K, Hayashi M, Nohmi T, Sawada M, and Matsuoka A. Primary mutagenicity screening of food additives currently used in

Japan. Food Chem Toxicol. **22**: 623–636. 1984.

22. Itoh K, Chiba T, Takahashi S, Ishii T, Igarashi K, Katoh Y, Oyake T, Hayashi N, Satoh K, Hatayama I, Yamamoto M, and Nabeshima Y. An Nrf2/small Maf heterodimer mediates the induction of phase II detoxifying enzyme genes through antioxidant response elements. Biochem Biophys Res Commun. **236**: 313–322. 1997.

23. Jaiswal AK. Regulation of genes encoding NAD(P)H:quinone oxidoreductases. Free Radic Biol Med. **29**: 254–262. 2000.

24. Kanki K, Umemura T, Kitamura Y, Ishii Y, Kuroiwa Y, Kodama Y, Itoh K, Yamamoto M, Nishikawa A, and Hirose M. A possible role of nrf2 in prevention of renal oxidative damage by ferric nitrilotriacetate. Toxicol Pathol. **36**: 353–361. 2008.

25. Kasai H, and Nishimura S. Formation of 8-hydroxydeoxyguanosine in DNA by oxygen radicals and its biological significance. In: Oxidative Stress: Oxidants and Antioxidants. H Sies. Academic Press, London. 99–116. 1991.

26. Kasai H, Nishimura S, Kurokawa Y, and Hayashi Y. Oral administration of the renal carcinogen, potassium bromate, specifically produces 8-hydroxydeoxyguanosine in rat kidney target organ DNA. Carcinogenesis. **8**: 1959–1961. 1987.

27. Kijima A, Ishii Y, Takasu S, Matsushita K, Kuroda K, Hibi D, Suzuki Y, Nohmi T, and Umemura T. Chemical structure-related mechanisms underlying in vivo genotoxicity induced by nitrofurantoin and its constituent moieties in gpt delta

rats. Toxicology. **331**: 125–135. 2015.

28. Kitamura Y, Umemura T, Kanki K, Kodama Y, Kitamoto S, Saito K, Itoh K, Yamamoto M, Masegi T, Nishikawa A, and Hirose M. Increased susceptibility to hepatocarcinogenicity of Nrf2-deficient mice exposed to 2-amino-3-methylimidazo[4,5-f]quinoline. Cancer Sci. **98**: 19–24. 2007.

29. Klaunig JE, Xu Y, Isenberg JS, Bachowski S, Kolaja KL, Jiang J, Stevenson DE, and Walborg EF Jr. The role of oxidative stress in chemical carcinogenesis. Environ Health Perspect. **106**: 289–295. 1998.

30. Kurokawa Y, Maekawa A, Takahashi M, and Hayashi Y. Toxicity and carcinogenicity of potassium bromate—a new renal carcinogen. Environ Health Perspect. **87**: 309–335. 1990.

31. Lau WL, Liu SM, Pahlevan S, Yuan J, Khazaeli M, Ni Z, Chan JY, and Vaziri ND. Role of Nrf2 dysfunction in uremia-associated intestinal inflammation and epithelial barrier disruption. Dig Dis Sci. **60**: 1215–1222. 2015.

32. Lee JS, and Surh YJ. Nrf2 as a novel molecular target for chemoprevention. Cancer Lett. **224**: 171–184. 2005.

33. Luan Y, Suzuki T, Palanisamy R, Takashima Y, Sakamoto H, Sakuraba M, Koizumi T, Saito M, Matsufuji H, Yamagata K, Yamaguchi T, Hayashi M, and Honma M. Potassium bromate treatment predominantly causes large deletions, but not GC>TA transversion in human cells. Mutat Res. **619**: 113–123. 2007.

34. Matsushita K, Ishii Y, Takasu S, Kuroda K, Kijima A, Tsuchiya T, Kawaguchi H, Miyoshi N, Nohmi T, Ogawa K, Nishikawa A, and Umemura T. A medium-term

gpt delta rat model as an in vivo system for analysis of renal carcinogenesis and the underlying mode of action. Exp Toxicol Pathol. **67**: 31–39. 2015.

35. Michaels ML, Pham L, Cruz C, and Miller JH. MutM, a protein that prevents G C→T A transversions, is formamidopyrimidine-DNA glycosylase. Nucleic Acids Res. **19**: 3629–3632. 1991.

36. Murata M, Bansho Y, Inoue S, Ito K, Ohnishi S, Midorikawa K, and Kawanishi S. Requirement of glutathione and cysteine in guanine-specific oxidation of DNA by carcinogenic potassium bromate. Chem Res Toxicol. **14**: 678–685. 2001.

37. Murata M, Midorikawa K, and Kawanishi S. Oxidative DNA damage and mammary cell proliferation by alcohol-derived salsolinol. Chem Res Toxicol. **26**: 1455–1463. 2013.

38. Nakabeppu Y. Cellular levels of 8-oxoguanine in either DNA or the nucleotide pool play pivotal roles in carcinogenesis and survival of cancer cells. Int J Mol Sci. **15**: 12543–12557. 2014.

39. Nohmi T, Kim SR, and Yamada M. Modulation of oxidative mutagenesis and carcinogenesis by polymorphic forms of human DNA repair enzymes. Mutat Res. **591**: 60–73. 2005.

40. Nohmi T, Suzuki T, and Masumura K. Recent advances in the protocols of transgenic mouse mutation assays. Mutat Res. **455**: 191–215. 2000.

41. O'Brien J, Renwick AG, Constable A, Dybing E, Müller DJ, Schlatter J, Slob W, Tueting W, van Benthem J, Williams GM, and Wolfreys A. Approaches to the

risk assessment of genotoxic carcinogens in food: a critical appraisal. Food Chem Toxicol. **44**: 1613–1635. 2006.

42. Okazaki K, Ishii Y, Kitamura Y, Maruyama S, Umemura T, Miyauchi M, Yamagishi M, Imazawa T, Nishikawa A, Yoshimura Y, Nakazawa H, and Hirose M. Dose-dependent promotion of rat forestomach carcinogenesis by combined treatment with sodium nitrite and ascorbic acid after initiation with N-methyl-N'-nitro-N-nitrosoguanidine: possible contribution of nitric oxide-associated oxidative DNA damage. Cancer Sci. **97**: 175–182. 2006.

43. Rossi L, Silva JM, McGirr LG, and O'Brien PJ. Nitrofurantoin-mediated oxidative stress cytotoxicity in isolated rat hepatocytes. Biochem Pharmacol. **37**: 3109–3117. 1988.

44. Rundhaug JE, and Fischer SM. Molecular mechanisms of mouse skin tumor promotion. Cancers. **2**: 436–482. 2010.

45. Saha SK, Lee SB, Won J, Choi HY, Kim K, Yang GM, Dayem AA, and Cho SG. Correlation between oxidative stress, nutrition, and cancer initiation. Int J Mol Sci. **18**: 1544. 2017.

46. Seitz HK, and Stickel F. Risk factors and mechanisms of hepatocarcinogenesis with special emphasis on alcohol and oxidative stress. Biol Chem. **387**: 349–360. 2006.

47. Small DM, Bennett NC, Roy S, Gabrielli BG, Johnson DW, and Gobe GC. Oxidative stress and cell senescence combine to cause maximal renal tubular epithelial cell dysfunction and loss in an in vitro model of kidney disease.

Nephron Exp Nephrol. **122**: 123–130. 2012.

48. Streeter AJ, and Hoener BA. Evidence for the involvement of a nitrenium ion in the covalent binding of nitrofurazone to DNA. Pharm Res. **5**: 434–436. 1988.

49. Suntres ZE, and Shek PN. Nitrofurantoin-induced pulmonary toxicity. In vivo evidence for oxidative stress-mediated mechanisms. Biochem Pharmacol. **43**: 1127–1135. 1992.

50. Tasaki M, Kuroiwa Y, Inoue T, Hibi D, Matsushita K, Kijima A, Maruyama S, Nishikawa A, and Umemura T. Lack of nrf2 results in progression of proliferative lesions to neoplasms induced by long-term exposure to non-genotoxic hepatocarcinogens involving oxidative stress. Exp Toxicol Pathol. **66**: 19–26. 2014.

51. Touati E, Phillips DH, Quillardet P, and Hofnung M. Determination of target nucleotides involved in 7-methoxy-2-nitro-naphtho[2,1-b]furan (R7000)-DNA adduct formation. Mutagenesis. **8**: 149–154. 1993.

52. Tsuchiya T, Kijima A, Ishii Y, Takasu S, Yokoo Y, Nishikawa A, Yanai T, and Umemura T. Role of oxidative stress in the chemical structure-related genotoxicity of nitrofurantoin in Nrf2-deficient gpt delta mice. J Toxicol Pathol. In press.

53. Umemura T, and Kurokawa Y. Etiology of bromate-induced cancer and possible modes of action-studies in Japan. Toxicology. **221**: 154–157. 2006.

54. Umemura T, Kai S, Hasegawa R, Kanki K, Kitamura Y, Nishikawa A, and Hirose M. Prevention of dual promoting effects of pentachlorophenol, an

environmental pollutant, on diethylnitrosamine-induced hepato- and cholangiocarcinogenesis in mice by green tea infusion. Carcinogenesis. **24**: 1105–1109. 2003.

55. Umemura T, Kanki K, Kuroiwa Y, Ishii Y, Okano K, Nohmi T, Nishikawa A, and Hirose M. In vivo mutagenicity and initiation following oxidative DNA lesion in the kidneys of rats given potassium bromate. Cancer Sci. **97**: 829–835. 2006.

56. Umemura T, Kitamura Y, Kanki K, Maruyama S, Okazaki K, Imazawa T, Nishimura T, Hasegawa R, Nishikawa A, and Hirose M. Dose-related changes of oxidative stress and cell proliferation in kidneys of male and female F344 rats exposed to potassium bromate. Cancer Sci. **95**: 393–398. 2004.

57. Umemura T, Kodama Y, Kurokawa Y, and Williams GM. Lack of oxidative DNA damage or initiation of carcinogenesis in the kidneys of male F344 rats given subchronic exposure to p-dichlorobenzene (pDCB) at a carcinogenic dose. Arch Toxicol. **74**: 54–59. 2000.

58. Umemura T, Kuroiwa Y, Kitamura Y, Ishii Y, Kanki K, Kodama Y, Itoh K, Yamamoto M, Nishikawa A, and Hirose M. A crucial role of Nrf2 in in vivo defense against oxidative damage by an environmental pollutant, pentachlorophenol. Toxicol Sci. **90**: 111–119. 2006.

59. Umemura T, Sai K, Takagi A, Hasegawa R, and Kurokawa Y. A possible role for cell proliferation in potassium bromate ($KBrO_3$) carcinogenesis. J Cancer Res Clin Oncol. **119**: 463–469. 1993.

60. van de Water B, Zoeteweij JP, and Nagelkerke JF. Alkylation-induced oxidative

cell injury of renal proximal tubular cells: involvement of glutathione redox-cycle inhibition. Arch Biochem Biophys. **327**: 71–80. 1996.

61. Wang Y, Gray JP, Mishin V, Heck DE, Laskin DL, and Laskin JD. Role of cytochrome P450 reductase in nitrofurantoin-induced redox cycling and cytotoxicity. Free Radic Biol Med. **44**: 1169–1179. 2008.

62. Yokoo Y, Kijima A, Ishii Y, Takasu S, Tsuchiya T, and Umemura T. Effects of Nrf2 silencing on oxidative stress-associated intestinal carcinogenesis in mice. Cancer Med. **5**: 1228–1238. 2016.

63. Zorzi RR, Jorge SD, Palace-Berl F, Pasqualoto KF, Bortolozzo Lde S, de Castro Siqueira AM, and Tavares LC. Exploring 5-nitrofuran derivatives against nosocomial pathogens: synthesis, antimicrobial activity and chemometric analysis. Bioorg Med Chem. **22**: 2844–2854. 2014.

英文要旨

Studies on the Role of Oxidative Stress in Mutagenesis by Using Nrf2-deficient Mice
（Nrf2 欠損マウスを用いた変異原性における酸化ストレスの役割に関する研究）

There are many chemical substances that are carcinogenic in the environment. The assessment of carcinogenesis risk in chemical substances ingested by humans through the diet is one of the most important issues for the public health. Oxidative stress is well known as a key factor in chemical-induced carcinogenesis. Nuclear factor erythroid 2-related factor 2 (NRF2) regulates cellular responses to oxidative stress and protects cells from them. Even though the actual role of oxidative stress in the carcinogenesis remains unclear, oxidative stress is considered to take a crucial role in renal carcinogenesis because that the kidney is exposed to many chemical substances during excretion and reabsorption, and redox cycles act vigorously accompanied with the production of reactive oxygen species (ROS) in the renal epithelial cells. Nitrofurantoin (NFT) and potassium bromate ($KBrO_3$) are chemical substances potentially ingested by humans through food. However, they both induce renal tumor in rats, and are prohibited or restricted in use currently for the concern about carcinogenesis risk in humans. Furthermore, they induce oxidative stress by the reduction of nitro group and the release of bromine radicals, respectively, and these oxidative stresses are suspected of relating to their renal carcinogenesis. 8-hydroxydeoxyguanosine (8-OHdG) is the most abundant oxidized DNA lesion induced by ROS, and is frequently used as a biomarker of oxidative stress in humans and experimental animals. Recently, it has been reported that the errors of 8-OHdG repair result in some types of gene mutation including transversion mutations and deletion mutations. In fact, our previous studies demonstrated that NFT and $KBrO_3$ increased the frequencies of different types of mutations: transversion mutations and deletion mutations, respectively with the elevation of 8-OHdG levels in the kidneys. Furthermore, the detailed relationship between oxidative stress or 8-OHdG and gene mutations induced by NFT or $KBrO_3$ remains unclear. *Gpt* delta rats and mice are the transgenic animal models which can detect *in vivo* mutagenicity in the target organs. Using these animals, 6-thioguanine and Spi^- selection can detect point mutation and deletion mutation, respectively. In addition, *Nrf2*$^{-/-}$ *gpt* delta mice created from *Nrf2*$^{-/-}$ mice and *gpt* delta mice is a new useful tool in the research for the role of oxidative stress in chemical-induced mutagenesis. Thus, in the present study, we investigate the involvement of oxidative stress in NFT or $KBrO_3$-induced *in vivo* mutagenicity using *Nrf2*$^{-/-}$ *gpt* delta mice.

NFT is synthesized by the condensation of 5-nitro-2-furaldehyde (NFA), a basic skeleton containing nitro group and 1-aminohydantoin as a side chain. In chapter 1, I performed reporter gene

mutation assays for NFT and NFA using *Nrf2*-proficient and -deficient *gpt* delta mice to clarify the role of oxidative stress in the chemical structure-related genotoxic mechanism of NFT. The mRNA expression level of *Nqo1* in the kidneys of vehicle-treated *Nrf2*$^{-/-}$ mice was significantly lower than that of vehicle-treated *Nrf2*$^{+/+}$ mice, consistent with the results observed for the protein expression of NQO1. Thus, our results confirmed that *Nrf2*$^{-/-}$ mice are hypersensitive to oxidative stress. *Gpt* MFs increased significantly with the elevation of 8-OHdG levels in the kidneys of *Nrf2*$^{-/-}$ mice orally administrated with NFT at a dose of 70 mg/kg, but not in *Nrf2*$^{+/+}$ mice. In particular, the rates of guanine base transversion mutations increased. NFA did not increase MFs of the reporter genes in the kidneys of both genotypes, despite the increase in 8-OHdG in NFA-treated *Nrf2*$^{-/-}$ mice. These results indicated the involvement of oxidative DNA damage in genotoxicity in the kidneys of NFT-treated *Nrf2*$^{-/-}$ mice, but not in the kidneys of NFA-treated *Nrf2*$^{-/-}$ mice, and the side chain interactions may affect the generation of oxidative stress by nitro-reduction of the nitro group.

In chapter 2, I performed reporter gene mutation assays and 8-OHdG measurements following $KBrO_3$ or NFT exposure using *Nrf2*-proficient and -deficient mice to clarify the relationship between $KBrO_3$- or NFT-induced oxidative stress and subsequent genotoxicity. In *Nrf2*$^{+/+}$ mice, the expression level of *Nqo1* was significantly increased by 4- or 13-week exposure to $KBrO_3$ and 13-week exposure to NFT despite of no increase in *Nrf2*$^{-/-}$ mice. The *Nqo1* expression levels of control, $KBrO_3$-treated, and NFT-treated *Nrf2*$^{-/-}$ mice were significantly lower than those of the corresponding *Nrf2*$^{+/+}$ mice. Thus, in the present study, *Nrf2*$^{-/-}$ mice were confirmed to be susceptible to oxidative stress. Four or thirteen-week administration of 1,500 ppm $KBrO_3$ in drinking water significantly increased the level of 8-OHdG and MFs in the kidneys of both genotypes. The degrees of increase of them are higher in *Nrf2*$^{-/-}$ mice than *Nrf2*$^{+/+}$ mice. In *Nrf2*$^{-/-}$ mice, the size of deletion was increased by $KBrO_3$ treatment. Four or thirteen-week administration of 2,500 ppm NFT in diet did not increase the level of 8-OHdG in the kidneys of either genotype. On the other hand, MFs were increased in the kidneys of 13-week NFT-treated animals of both genotypes, and the degrees of increase of MFs are higher in *Nrf2*$^{-/-}$ mice than *Nrf2*$^{+/+}$ mice. These results suggested that the formation of 8-OHdG, which resulted from the oxidizing potential of $KBrO_3$, was directly involved in the increase of deletion mutations; however, oxidative stress-related factors other than 8-OHdG might play a critical role in NFT-induced guanine base substitution mutations.

In conclusion, I demonstrated the different modes of involvement of oxidative stress in the mutagenesis induced by NFT or $KBrO_3$ using *Nrf2*$^{-/-}$ *gpt* delta mice which showed high sensitivity to oxidative stress. In NFT-induced mutagenesis, the side chain interactions may affect the generation of oxidative stress by nitro-reduction of the nitro group, then the oxidative stress-related factors other than 8-OHdG might play a critical role in NFT-induced guanine base substitution mutations. In $KBrO_3$-induced mutagenesis, the formation of 8-OHdG, which resulted from the oxidizing potential of $KBrO_3$, was directly involved in the increase of deletion mutations. From my findings, it was also

suggested that the impact of the formation of 8-OHdG was clearly different in each chemical substance considering the risk assessment of oxidative stress, and investigations about the detailed mechanisms including oxidative stress seem to be necessary in the risk assessment of environmental chemical substances. Even though how nitro group and side chain in nitrofurans interact in the induction of oxidative stress and what kinds of repair errors act in the induction of deletion mutations by $KBrO_3$ remain unclear, the present study contributes to accurate risk assessment of oxidative stress in carcinogenicity by environmental chemical substances, and I will further progress research about oxidative stress.

和文要旨

Studies on the Role of Oxidative Stress in Mutagenesis by Using Nrf2-deficient Mice
（Nrf2 欠損マウスを用いた変異原性における酸化ストレスの役割
に関する研究）

環境中には多くの発がん物質が存在し，私達は常にそれらの曝露の危険にさらされている。 食品を介してヒトが摂取する可能性のある化学物質の発がんリスク評価は，公衆衛生上最も重要な問題の１つである。また，それらにより誘発される酸化ストレスは，化学発がん過程において重要な役割を担うことが知られており，生体内では転写因子の１つである NRF2 が抗酸化酵素群の発現調節を介して酸化ストレス防御に重要な役割を担う。腎臓は様々な物質の排泄や再吸収過程を担うが，尿細管上皮はその際の盛んな酸化還元反応で生じる活性酸素種（ROS）による酸化ストレスの影響を強く受ける。またげっ歯類における腎発がんに対する酸化ストレスの関与を示唆されており，ヒトにおいても同様のリスクが懸念される。ニトロフラントイン（NFT）および臭素酸カリウム（$KBrO_3$）はそれぞれ残留農薬および食品添加物としてヒトが摂取する可能性のある化学物質であるが，いずれもラットにおいて腎発がん性が報告されている。また，両者はそれぞれニトロ基の還元反応およびブロミンラジカルの生成を介して酸化ストレスを誘発するため，その発がん性への酸化ストレスの関与が疑われている。ROS により形成される最も代表的な酸化的 DNA 損傷の１つである 8-OHdG は，ヒトの臨床現場や実験動物において酸化ストレスマーカーとして広く用いられているが，近年その修復過程で生じるエラーが様々な種類の遺伝子変異につながることが報告されている。実際に NFT と $KBrO_3$ は，腎臓において 8-OHdG の増加を伴って遺伝子変異頻度（MFs）を増加させるが，それらが誘導する主要な変異パターンはそれぞれ transversion 変異と欠失変異と異なっている。*Gpt* delta ラットおよびマウスは *gpt* あるいは Spi⁻アッセイにより点突然変異や欠失変異を検出可能な遺伝子改変動物モデルであり，これと *Nrf2* 欠損マウスから作出された *Nrf2*$^{-/-}$ *gpt* delta マウスは化学物質による変異原性における酸化ストレスの関与を検討出来る新たな動物モデルである。そこで本研究では，酸化ストレスに高感受性でありかつ対象臓器における *in vivo* 変異原性を検出出来る動物モデルである *Nrf2*$^{-/-}$ *gpt* delta マウスを用いて両剤による変異原性における酸化ストレスの関与を検討した。

第１章では，NFT における化学構造依存的な遺伝毒性機序における酸化ストレスの役割を明らかにするため，NFT とニトロ基を有するその基本骨格である 5-nitro-2-furaldehyde（NFA）について，*Nrf2*$^{+/+}$および *Nrf2*$^{-/-}$ *gpt* delta マウスを用いて遺伝子変異解析を実施した。NRF2 制御下の抗酸化酵素である NQO1 は，その遺伝子およびタンパク発現レベルが *Nrf2*$^{-/-}$マウスにおいて *Nrf2*$^{+/+}$マウスよりも顕著に少なく，*Nrf2*$^{-/-}$

gpt delta マウスは酸化ストレスに対して高感受性であることが確認された。このような条件下で，NFT を 70 mg/kg の用量で経口投与した *Nrf2*$^{-/-}$マウスでは，8-OHdG の増加を伴って MFs が増加し，この時グアニン塩基における transversion 変異が主体であった。一方，NFA は 8-OHdG を増加させたが MFs は増加させなかった。これらのことから，NFT による遺伝毒性に酸化ストレスは関与するが NFA による遺伝毒性には関与しないこと，およびニトロ基の還元反応による酸化ストレスの発生に側鎖との相互反応が影響していることが示唆された。

第２章では，$KBrO_3$ および NFT により誘発される酸化ストレスとそれに続く遺伝子変異の関連を明らかにするため，$KBrO_3$ と NFT について同様に遺伝子変異解析および 8-OHdG 測定を実施した。*Nqo1* の発現レベル解析において，*Nrf2*$^{+/+}$マウスでは両者の投与によりその発現が顕著に増加したのに対し，*Nrf2*$^{-/-}$マウスでは変化がみられず，投与の有無にかかわらず *Nrf2*$^{+/+}$マウスよりも低値を示した。このように *Nrf2*$^{-/-}$ *gpt* delta マウスは第１章と同様に酸化ストレスに強くさらされていることが確認された。このとき，$KBrO_3$ の 1,500 ppm での飲水投与により 8-OHdG の増加を伴って欠失変異を主体として MFs が顕著に増加し，その増加の程度は *Nrf2*$^{-/-}$において *Nrf2*$^{+/+}$よりも大きく，*Nrf2*$^{-/-}$マウスでは欠失サイズの増加もみられた。一方 NFT の 2,500 ppm での混餌投与では 8-OHdG の増加を伴わずにグアニン塩基における transversion 変異を主体として MFs の増加がみられ，この時もその増加の程度は *Nrf2*$^{-/-}$において *Nrf2*$^{+/+}$よりも大きいことが明らかになった。これらのことから，$KBrO_3$ の強い酸化力に起因する 8-OHdG 形成は直接的に欠失変異の増加に関与していることが示唆され，一方で NFT によるグアニン塩基における transversion 変異には 8-OHdG 以外の酸化ストレス因子が関与している可能性が考えられた。

Nrf2$^{-/-}$ *gpt* delta マウスを用いた本研究の結果から，NFT および $KBrO_3$ による変異原性において酸化ストレスがそれぞれ異なる関与の様式を示すことが明らかになった。このように，酸化ストレスに関するリスク評価において 8-OHdG 形成が及ぼす影響の大きさは化学物質ごとに異なると考えられる。また，酸化ストレスを含む詳細な発がん機序の検討が環境中の化学物質による発がんリスク評価には重要である。本研究の成果は化学発がんにおける酸化ストレスについてのより正確なリスク評価に貢献するものであり，酸化ストレスに関する更なる研究を進めていきたい。